CHAPTER IV

RESULTS, ANALYSES AND DISCUSSIONS

4.1 Effect of Fly Ash on Plastic Shrinkage Cracking of Concrete

4.1.1 Properties

Table 4.1 lists the properties observed from the fly ash concrete specimens. As expected, the workability and cohesiveness of the concrete improved as the amount of fly ash increased and placement of the fresh concrete unto the panel formworks was easier as both the water-binder ratio and fly ash content increased. The slump recorded increased with the amount of fly ash. This behavior was attributed to the ball bearing effect of fly ash due to its spherical shape and plain surface which acts like lubricant that enhances mobility.

After determining setting times from specimens exposed to the required environmental conditions (that produces the 1.0 $kg/m^2 \cdot h$ minimum evaporation rate), it was found that increasing the fly ash content made the setting time longer than that of the control specimens. Retardation of the setting time due to fly ash may be affected by the proportion or amount, fineness, and chemical composition of the said pozzolan.

In terms of the 28^{th} day compressive strength, the values for fly ash concrete were lower than the compressive strength of the control specimens. This exhibited that the use of fly ash as a partial replacement for cement would result to lower compressive strength at early ages. Low strength development of fly ash concrete at early ages was presumably a consequence of decreased cement content rather than slower hydration and pozzolanic reaction (Jawed and Skalny, 1981).

Table 4.1: Properties of fly ash concrete

Designation	w/b ratio	Fly Ash Used	Time of Setting		Slump	Compressive Strength (28-day)
			Initial	Final		
w/b-%FA	w/b	%FA	hr:min	hr:min	cm	ksc
30-C	0.30	0	2:10	2:55	5.0	465
30-10FA		10	3:40	4:55	6.0	446
30-30FA		30	3:45	5:00	7.0	407
30-50FA		50	4:20	5:45	16.5	403
40-C	0.40	0	3:10	4:25	9.0	444
40-10FA		10	3:15	4:50	11.0	376
40-20FA		20	4:00	5:25	12.5	361
40-30FA		30	4:00	5:25	19.5	352
40-40FA		40	4:45	6:10	21.5	344
40-50FA		50	4:45	6:10	23.5	284
50-C	0.50	0	3:30	4:40	13.5	335
50-10FA		10	3:55	5:25	16.0	314
50-30FA		30	4:15	5:45	20.0	293
50-50FA		50	4:45	6:30	22.0	233

C = Control Specimen FA = Fly Ash w/b = Water/Binder Ratio

The appearance of the first crack in the specimens could be seen in Table 4.2. The delay in the appearance of cracks as the fly ash content increased was believed to be due to the availability of the bleed water (Bouzoubaa, Bilodeau, Sivasundaram, Fournier, Golden, 2004). Once all of the bleed water evaporated, only then would the cracks begin to appear. The delay in crack appearance might also probably due to the fine pore structure and low rate of bleeding water in low water/binder ratio pastes which would generate high capillary pressure in the mix (Wang, Shah, Phuaksuk, 2001).

No crack appeared in the specimens for the 50-50FA mix, thus no value was placed in Table 4.2. This behavior would be further explained in the next section of this chapter.

Table 4.3 contained the recorded evaporation rate and environmental conditions (wind velocity, temperature, and relative humidity) taken as the average values throughout the whole testing duration. The wind velocity was constant at 4.0 m/s since the fan speed of the fan installed in the test chamber was non-adjustable. The heater dial settings were adjusted as needed in order to somehow control the temperature to be able to obtain the required minimum evaporation rate. The average

evaporation rate ranged from 1.01 kg/m^2·h to 1.09 kg/m^2·h. It was a bit challenging to maintain a 1.0 kg/m^2·h throughout the testing duration since testing was done inside the laboratory and not in a controlled room, thus explains the varying values for temperature and relative humidity.

Table 4.2: Time of appearance of first crack in fly ash concrete specimens

Designation	Time of Crack Appearance
w/b-%FA	min
30-C	60
30-10FA	60
30-30FA	90
30-50FA	120
40-C	90
40-10FA	90
40-20FA	90
40-30FA	90
40-40FA	120
40-50FA	120
50-C	90
50-10FA	120
50-30FA	120
50-50FA	NA

Table 4.3: Evaporation rate and environmental conditions during testing of fly ash specimens

Designation	Evaporation Rate	Wind Velocity	Temperature	Relative Humidity
w/b-%FA	kg/m^2/h	m/s	°C	%
30-C	1.01	4.0	36.0	31
30-10FA	1.07	4.0	37.0	35
30-30FA	1.05	4.0	37.0	38
30-50FA	1.08	4.0	37.0	37
40-C	1.08	4.0	33.5	29
40-10FA	1.07	4.0	37.0	40
40-20FA	1.07	4.0	34.5	30
40-30FA	1.08	4.0	39.0	35
40-40FA	1.06	4.0	34.5	33
40-50FA	1.09	4.0	34.5	33
50-C	1.06	4.0	36.5	46
50-10FA	1.09	4.0	37.0	31
50-30FA	1.07	4.0	34.5	29
50-50FA	1.08	4.0	35.5	27

4.1.2 Effect on Average Crack Width

Histograms plots of the measured crack widths from all three specimens per concrete mix are presented in Figures 4.1 to 4.3. The 20 interval range of crack width values (horizontal axis) was automatically generated by SPSS for Windows. Based on the statistical parameters from the measured data in Table 4.4, the crack widths were normally distributed. The mean and median values had very little difference which indicated that the distribution was symmetrical. The value of the mode would not be determined from the generated histogram as it was determined from the recorded measured widths with the most number of occurrences (per single measured value) and the histogram shows the accumulated frequencies per range. The mode, like the mean and median, increased as the amount of fly ash increased. Also, it is observed that the mode was a bit less than the mean. This could indicate that the crack width that would transpire the most would be a little less than the average crack width. The variations of measured crack width were also small as shown by the small variance values.

Table 4.4: Statistical parameters of fly ash concrete crack widths

Designation	Data Points	Mean	Median	Mode	Variance	Standard Deviation
w/b-%FA	-	mm	mm	mm	mm	mm
30-C	207	0.593	0.570	0.49	0.053	0.231
30-10FA	170	0.647	0.620	0.50	0.056	0.237
30-30FA	217	0.611	0.600	0.40	0.052	0.227
30-50FA	203	0.638	0.600	0.56	0.074	0.271
40-C	160	0.591	0.570	0.78	0.034	0.185
40-10FA	159	0.562	0.530	0.35	0.039	0.197
40-20FA	166	0.561	0.510	0.43	0.047	0.216
40-30FA	198	0.592	0.550	0.78	0.047	0.216
40-40FA	172	0.592	0.590	0.59	0.592	0.243
40-50FA	135	0.681	0.670	0.73	0.043	0.208
50-C	192	0.708	0.640	0.77	0.084	0.289
50-10FA	178	0.662	0.610	0.61	0.051	0.225
50-30FA	70	0.627	0.620	0.62	0.022	0.150

It should be noted that the tabulated average or mean crack widths exceeded the tolerable crack widths for different exposure conditions as suggested by ACI 224R

(Control of Cracking in Concrete Structures), shown in Table 4.5. This could imply that necessary precautions if the same mix proportions would be used, and if subjected to sufficient restraints and similar environmental conditions as tested, must be implemented in order for resulting plastic shrinkage crack to be invulnerable to permeability or damage due to exposure conditions.

Table 4.5: Tolerable crack widths for different exposure conditions (ACI 224R)

Exposure Condition	Tolerable Crack Width
	Mm
Dry air / protective membrane	0.41
Humidity, moist air, soil	0.30
Deicing chemicals	0.18
Seawater and seawater spray; wetting and drying	0.15
Water retaining structure (excluding nonpressure pipes)	0.10

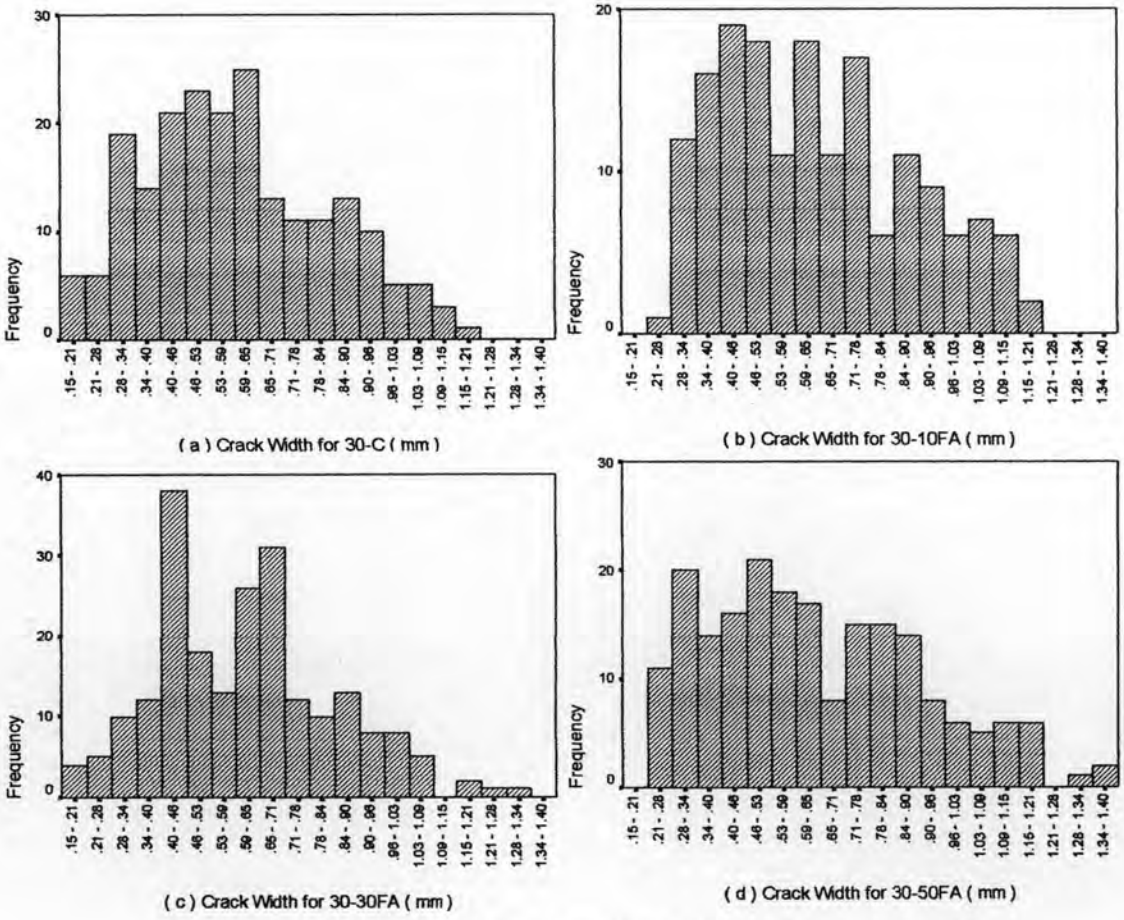

Figure 4.1: Histogram plots of crack widths of fly ash concrete specimens with w/b = 0.30

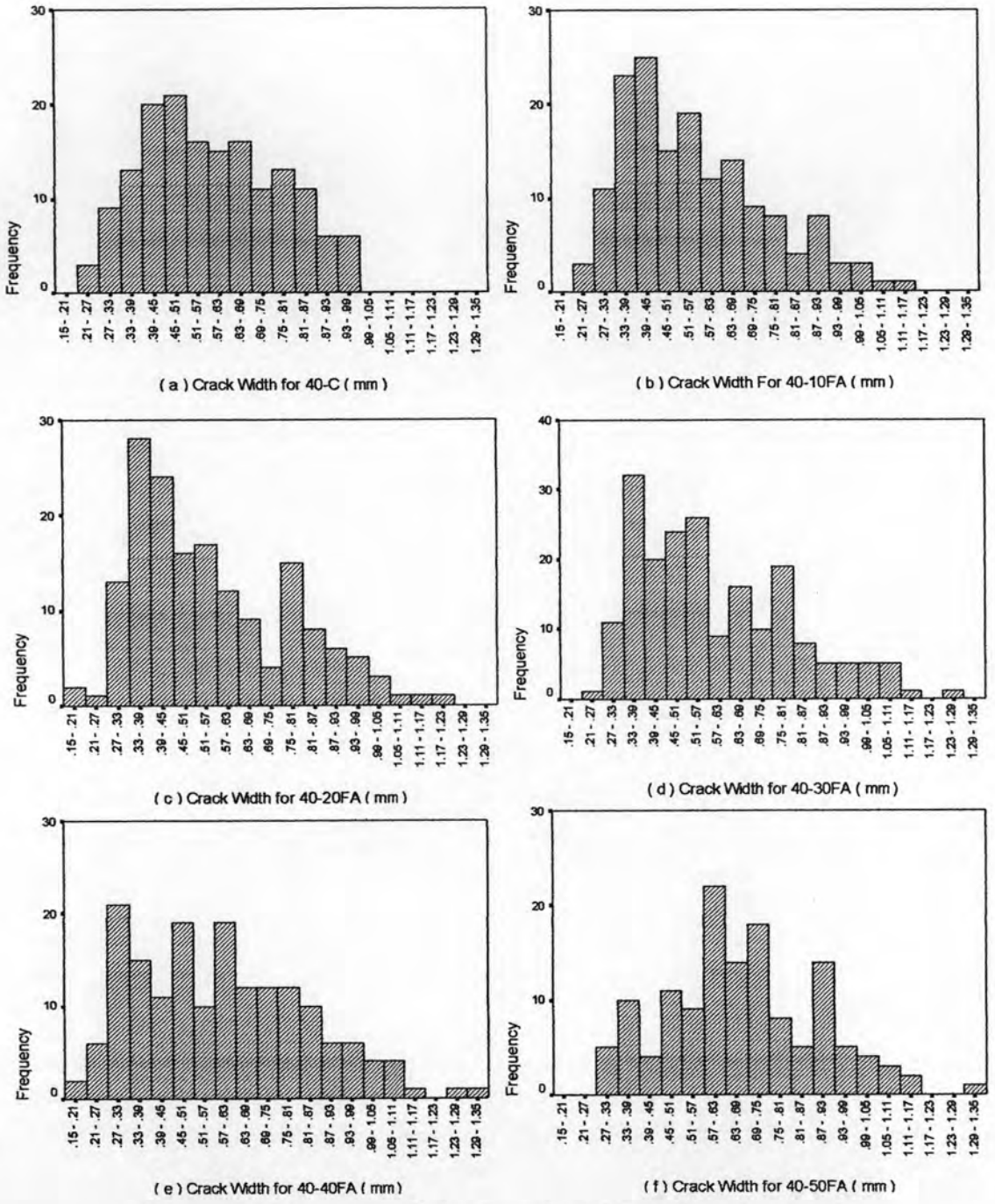

Figure 4.2: Histogram plots of crack widths of fly ash concrete specimens with w/b = 0.40

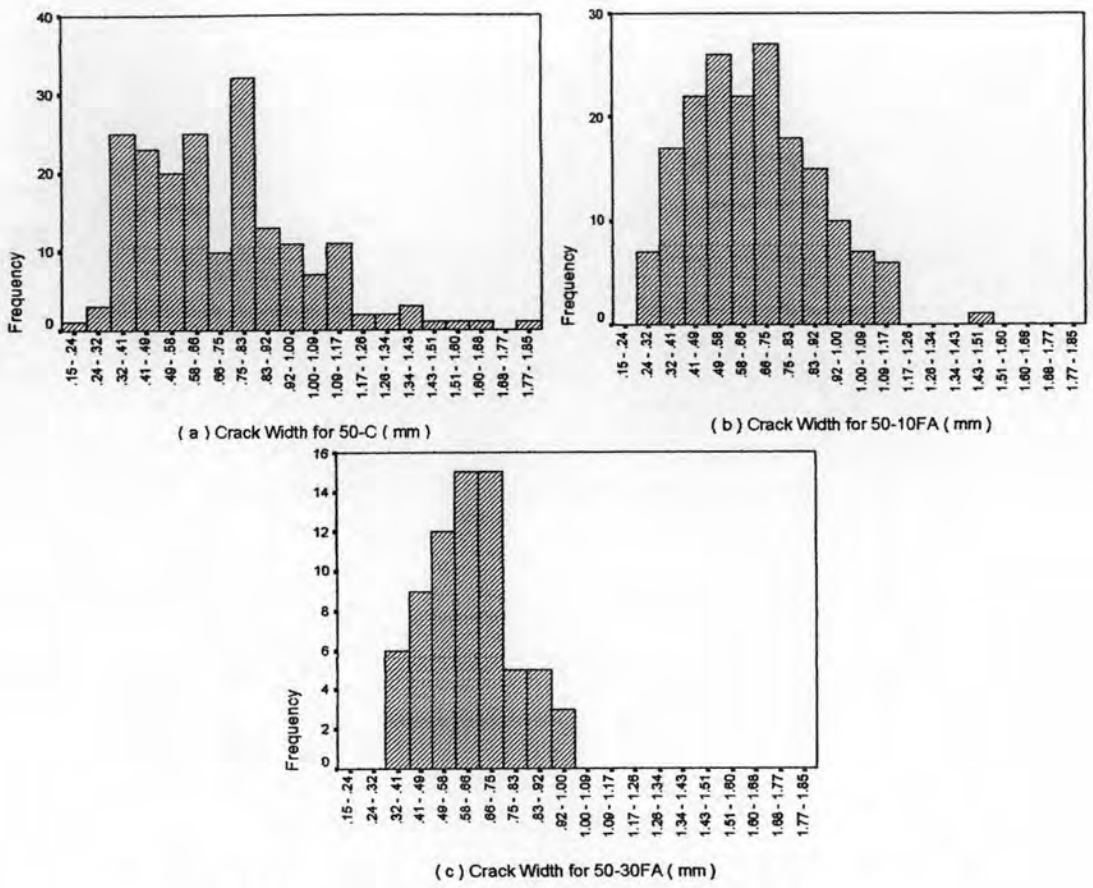

Figure 4.3: Histogram plots of crack widths of fly ash concrete specimens with w/b = 0.50

It was observed that fly ash concrete specimens with water/binder ratios of 0.30 and 0.40 behaved similarly and specimens with 0.50 water/binder ratio behaved otherwise. Normal distribution curves of the measured crack widths from concrete specimens with 0 to 50 percent cement replacement by fly ash could be seen in Figures 4.4 to 4.6. The horizontal axis points represent the midpoint crack width value of the 20 interval range automatically generated by SPSS for Windows. Relative to the peak of the normal distribution curve of the control (0% fly ash replacement), the curves based on the crack widths from specimens with water/binder ratios of 0.30 and 0.40 (Figures 4.4 and 4.5, respectively) were a little bit displaced to the right as the amount of fly ash increased. This indicates an increase in average crack width as the amount of fly ash increased. However, the normal distribution curves of specimens with water/binder ratio of 0.50 (Figure 4.6) shifted to the left which indicated a decrease in average crack width with the increase of fly ash content in concrete.

Standard deviation describes the shape of the normal distribution curves in terms of the spread of values with respect to the mean. From Table 4.4, the standard deviation values tend to increase as the fly ash content increased for specimens using water/binder ratios of 0.30 and 0.40. This signified that the distribution of the crack width values tend to be further from the mean value, which is also shown by the wider shape of the distribution curve. On the other hand, the crack width distribution of specimens with water/binder ratio of 0.50 had standard deviation values that decreased as the amount of fly ash increased. Smaller standard deviation values results in narrower distribution curves which indicated that the specimens had a more uniform distribution of crack width. This was because most of the recorded crack width values were close to the mean value.

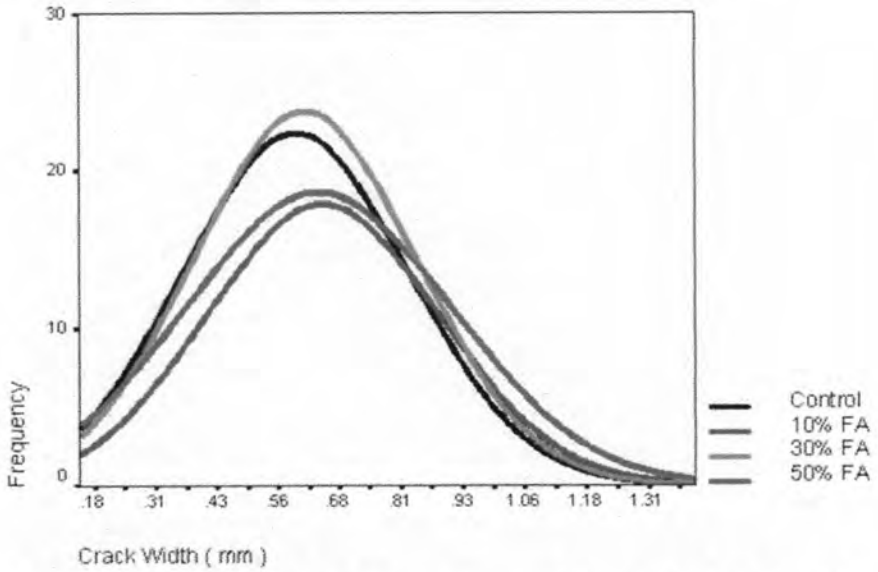

Figure 4.4: Normal distribution curves of crack width of fly ash concrete specimens with water/binder ratio = 0.30

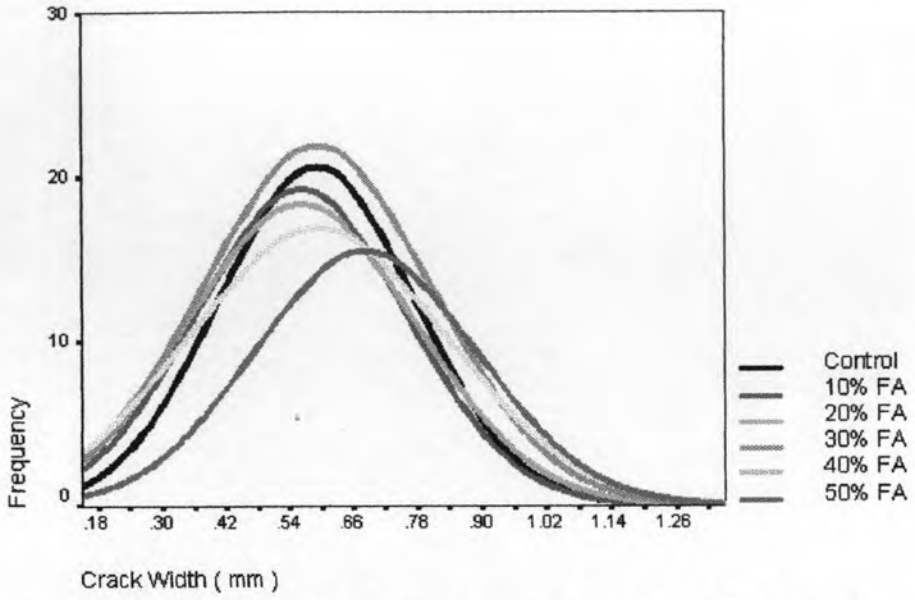

Figure 4.5: Normal distribution curves of crack width of fly ash concrete specimens with water/binder ratio = 0.40

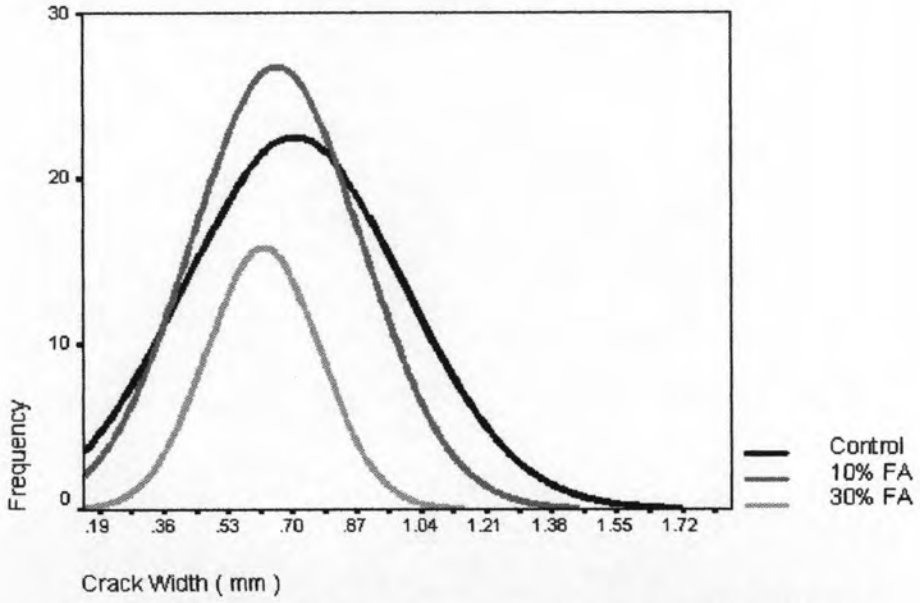

Figure 4.6: Normal distribution curves of crack width of fly ash concrete specimens with water/binder ratio = 0.50

In order to further support these findings, other statistical tests were done. Linear regression modeling of calculated average crack width values has shown relatively higher significance than other statistical models. Results from linear regression (Figure 4.7) have shown the same trend as what was observed from the normal distribution curves. Note that these results show only the trend or the tendency

of the influence of fly ash on plastic shrinkage cracking (in terms of average crack width in this section and maximum crack width, crack area, and cracking reduction ratio to follow).

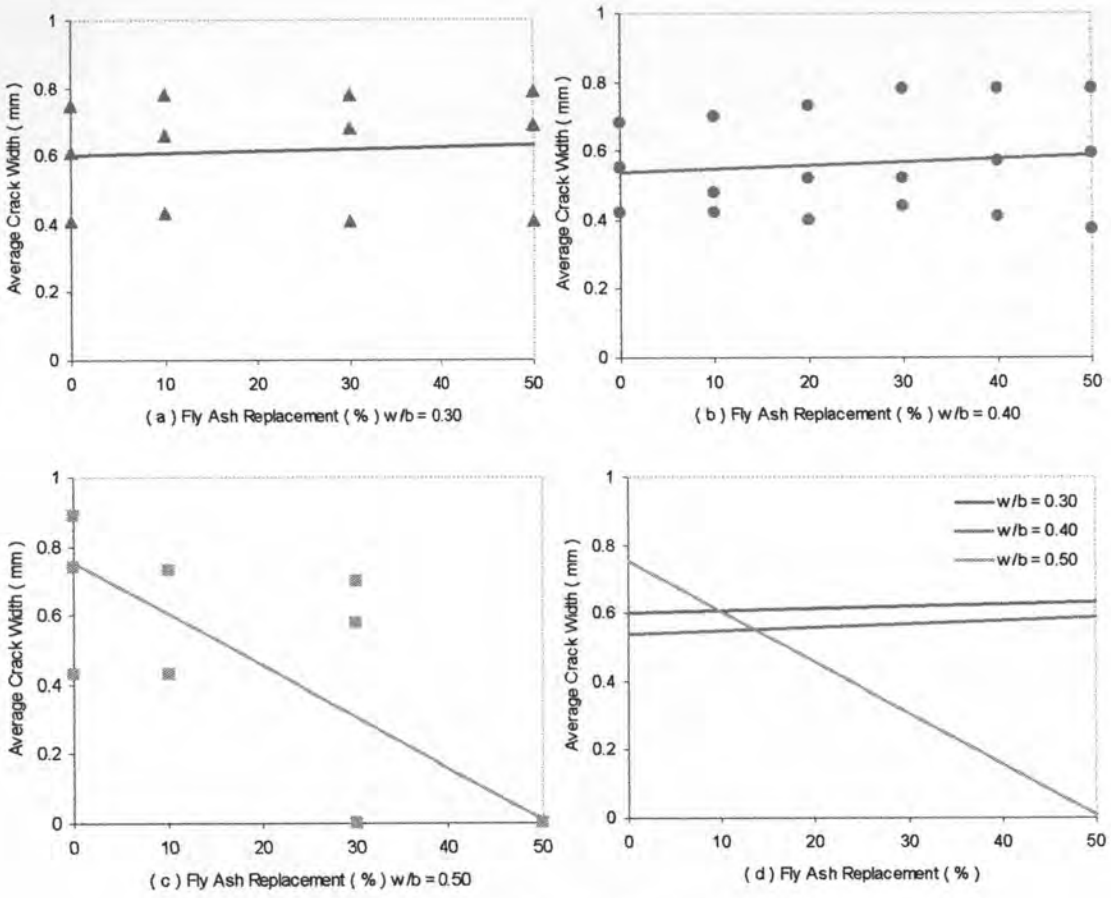

Figure 4.7: Effect of fly ash content on average crack width

An increase in the average crack width was noticed as the amount of fly ash increased for specimens using water/binder ratios of 0.30 and 0.40 which was similar to the results of Stitmannaithum, Raksamata, and Chalanun (2002). This might due to the fact that for such low water/binder ratios, increasing the amount of fly ash could decrease the amount of bleed water which, in turn, increases the plastic shrinkage (Bouzoubaa, Bilodeauu, Sivasundaram, Fournier, and Golden, 2004).

The value of the average crack width for both specimens with 0.30 and 0.40 water/binder ratios seem to be almost constant at 10% fly ash replacement. Such slight change in behavior was also seen previously in the normal distribution curves in

Figures 4.4 and 4.5. This could imply that use of 10% fly ash replacement in concrete with water/binder ratios of 0.30 or 0.40 could possibly not render any change as compared to control mixes

A significant decrease in average crack width would be observed from specimens using 0.50 water/binder ratio. This decrease was attributed to the observed increase in the amount of bleed water that was available at the surface of the specimen as the amount of fly ash increased. In this case, since the water content for all mixes were constant and the use of fly ash reduces water requirement then there would be a considerable amount of bleed water that could rise to the surface of the specimens. Once all of the bleed water have evaporated, only then would the cracks start to appear. Still, since crack formation was delayed then it could be the cause for the possible delay in further widening of the cracks thus leading to lesser crack width values than that of specimens with water/binder ratio of 0.30 and 0.40.

It was observed that all three specimens of 50-50FA mix did not have any cracks at all. Throughout the duration of testing the 50-50FA specimens, it was seen that there was a lot of bleed water that rose to the surface of the specimen and it took a long time until all bleed water at the surface dried out. In order to justify such behavior, the bleed rate of the 50-50FA concrete mix was determined. It was found that for the first thirty minutes, the bleed rate was 17.66 $kg/m^2 \cdot h$. Such value is indeed greater than the measured evaporation rate of 1.08 $kg/m^2 \cdot h$ after thirty minutes from the start of the test. For the first ten minutes of testing, the bleed rate was 31.49 $kg/m^2 \cdot h$ as compared to the evaporation rate of 0.97 $kg/m^2 \cdot h$. Based on this, it was believed that the reason behind the non-appearance of cracks for 50-50FA specimens was that the bleed rate was far greater than the evaporation rate for plastic shrinkage to occur. This result was in agreement with a similar study done by Wang, Shah, Phuaksuk (2001) using water/binder ratio of 0.55 with fly ash contents of 0, 30, and 50%.

4.1.3 Effect on Maximum Crack Width

The behavior of the trends of measured maximum crack widths was similar to that the observed trends of the calculated average crack widths from linear regression analysis as shown in Figure 4.8. Once again, the maximum crack width increased as the fly ash content was also increased for specimens with 0.30 and 0.40 water/binder ratio. It is also noticeable that 10% replacement of fly ash in concrete for both 0.30 and 0.40 water/binder ratio rendered almost constant maximum crack width values with control specimens. For specimens with water/binder ratio of 0.50, maximum crack width decreased as the fly ash content decreased. These trends occur due to the same reasons as that stated in the previously discussed section.

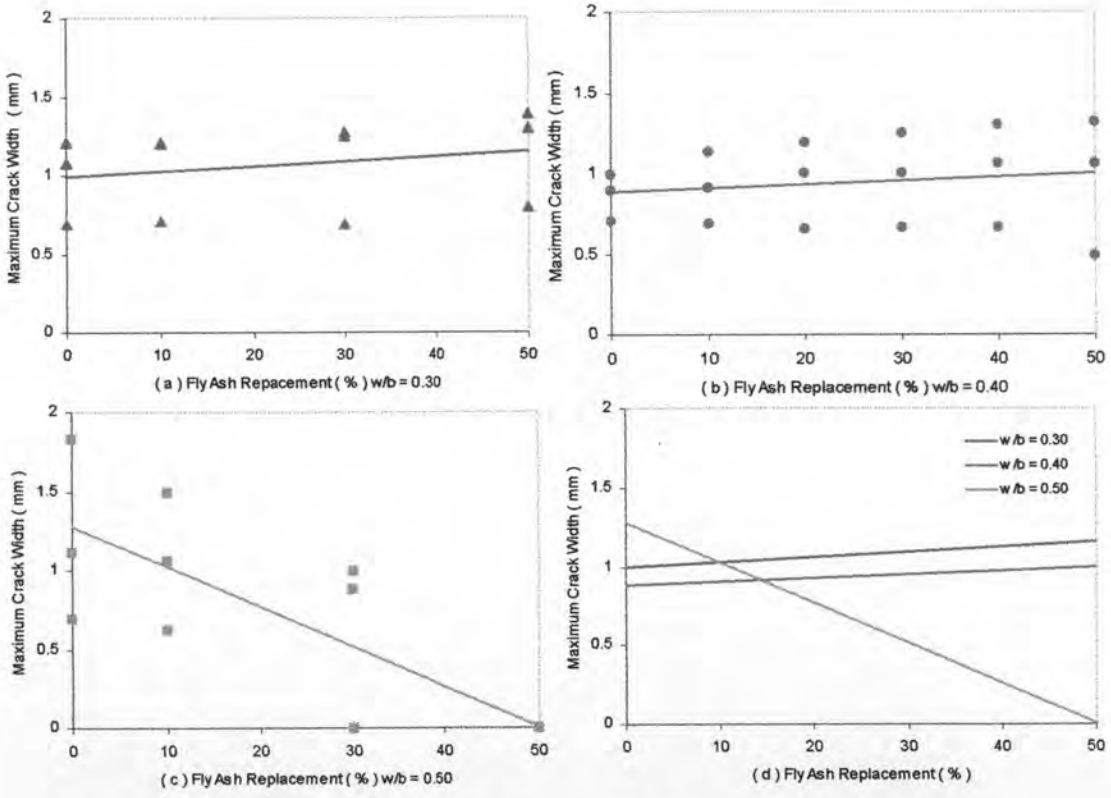

Figure 4.8: Effect of fly ash content on maximum crack width

Ninety percentile crack width values were determined from the measured crack widths. In doing so, two methods of approach were used for comparison. From the normal distribution curves previously shown (Figures 4.4 to 4.6), the value at the 90 percentile mark was obtained per mix proportion. The other approach was done by

sorting the measured crack widths from all three specimens per fly ash concrete mix in ascending order having the least value as x_1 and the greatest value as x_n. From the n number of total measurements, the limiting crack width value per mix proportion from this method was $x_{(0.90\,n)}$. As seen in Table 4.6, there were some slight differences between the resulting values of the two methods which could attest to the normal distribution of the measured crack widths. This indicated that when the following mix proportions are used, 90 percent of the plastic shrinkage crack widths would not exceed the tabulated values. However, it must be noted that these values still exceeded the tolerable crack widths suggested by ACI 224R (Table 4.5) for different exposure conditions. Because of this, extreme care must still be implemented in using fly ash concrete in terms of plastic shrinkage crack widths.

Table 4.6: Ninety percentile crack width values of fly ash concrete specimens

Designation	90 Percentile Crack Width Values	
	Normal	Sort
w/b-%FA	mm	mm
30-C	0.92	0.92
30-10FA	0.98	0.97
30-30FA	0.95	0.95
30-50FA	1.02	1.00
40-C	0.85	0.84
40-10FA	0.88	0.84
40-20FA	0.90	0.87
40-30FA	0.89	0.89
40-40FA	0.95	0.93
40-50FA	0.96	0.94
50-C	1.09	1.09
50-10FA	0.96	0.96
50-30FA	0.85	0.85

4.1.4 Effect on Crack Area

From the previous two sections, it was inferred that the use of fly ash seemed to increase plastic shrinkage crack widths. However, calculations of plastic shrinkage crack area of specimens have shown a corresponding decrease in values as the amount of fly ash used in concrete increased. The trend could be observed in Figure 4.9.

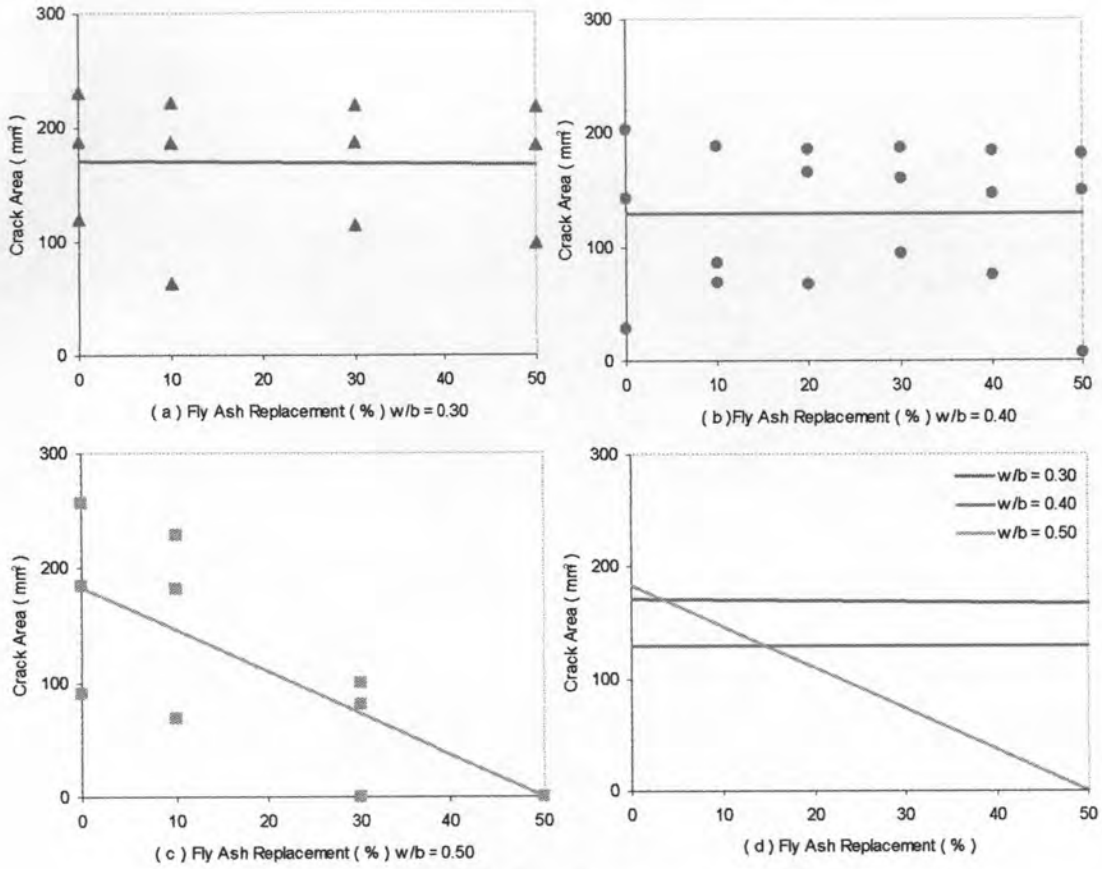

Figure 4.9: Effect of fly ash content on crack area

From Figure 4.9, it is seen that crack area was greater in the stiffer mix with water/binder ratio of 0.30 than in specimens using 0.40 water/binder ratio. However, the crack area values of specimens with water/binder ratio of 0.30 were almost constant since it exhibited only a slight decrease in values. Also, crack area seemed to decrease as workability increased (which is also due to the increased amount of fly ash content). Such observations were in direct agreement with the theory of the effect of paste stiffness on plastic shrinkage crack area (Wang, Shah, Phuaksuk, 2001). The less workable the mix was, the greater crack area it would have. Since the use of fly ash in concrete enhances workability, hence improving cohesion of the paste, then it could lead to the decrease in the crack area.

It could be noticed that the crack area of the specimens using high water/binder ratio of 0.50 had greatly decreased. This might be partially due to the relatively large pore size of the paste which reduces pore pressure (Wang, Shah, Phuaksuk, 2001). Since there were no cracks that appeared in mixes with 50 percent

replacement of cement by fly ash using 0.50 water/binder ratio, then it follows that the value of crack area for the said mix would be zero. This was reflected in Figure 4.9 as the regression line crossed the zero crack area mark at 50% fly ash replacement. Such behavior was also in accord with results from tests done by Wang, Shah, Phuaksuk (2001) using fly ash contents of 0, 30, and 50% having a decreasing trend for crack area with respect to fly ash content at a high water/binder ratio of 0.55.

Figure 4.10 presents a more general trend of crack area against the amount of fly ash used in the concrete mix. Such behavior was also observed by Stitmannaithum, Raksamata, and Chalanun (2002). Linear regression analysis was preformed using all calculated crack area values irregardless of which water/binder ratio was used. The decrease in crack area was also due to the filling effect due to the fineness of fly ash particles. The particle size of fly ash served as excellent fillers for the void space within aggregates. The smooth surface and spherical shape of fly ash particles also reduced interparticle friction which improved mobility and cohesion. Also, it was observed that the crack formed became more discontinuous as the amount of fly ash used increased. The discontinuity of the cracks resulted in shorter crack length which, in turn, decreases the calculated crack area of the specimen.

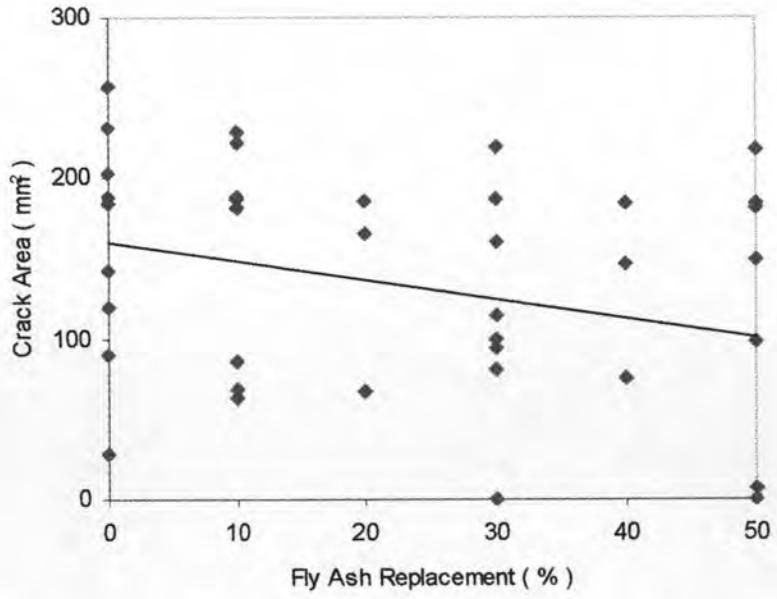

Figure 4.10: General effect of fly ash content on crack area

4.1.5 Effect of Curing on Fly Ash Concrete

Curing could be one of the tools into further reducing plastic shrinkage cracking in concrete. Its effects on fly ash concrete would vary depending on which curing condition would be used to expose the specimens. Changes after curing were compared to the crack quantification values of the chosen specimen from the start of the test.

As mentioned in the previous chapter, one specimen per curing condition would be investigated. The number of crack width measurements per specimen was noted before and after exposure to curing, as shown in Table 4.7. Normal distribution curves of the measured crack widths of specimens chosen to undergo curing for 28 days are shown in Figures 4.11 to 4.16. It was observed from these figures that the normal distribution curve shifts to the left after undergoing 28 of curing. This indicated the ability of concrete to heal itself due to further pozzolanic reactions. Also, such behavior has shown that the crack widths decreased after undergoing 28 days of either air curing or moist curing by wet burlap.

Table 4.7: Number of crack width measurements of fly ash concrete specimens for curing

Designation	Number of Data Points			
	Air Curing		Moist Curing	
	Day 1	Day 28	Day 1	Day 28
30-C	73	68	67	66
30-10FA	66	64	64	62
30-30FA	70	65	69	64
30-50FA	63	52	75	66
40-C	66	58	72	69
40-10FA	52	44	69	68
40-20FA	69	63	57	56
40-30FA	67	60	74	67
40-40FA	62	57	58	55
40-50FA	64	62	67	60
50-C	64	63	71	68
50-10FA	62	61	75	65
50-30FA	33	26	43	35

Interestingly, specimens with water/binder ratio of 0.30 and 0.40 that was exposed to air curing conditions exhibited slight movement (to the left) after curing as shown in Figures 4.11 and 4.13. However, greater displacement was seen after moist curing (Figures 4.12 ad 4.14). This indicated the effectiveness of moist curing in further reducing plastic shrinkage crack widths.

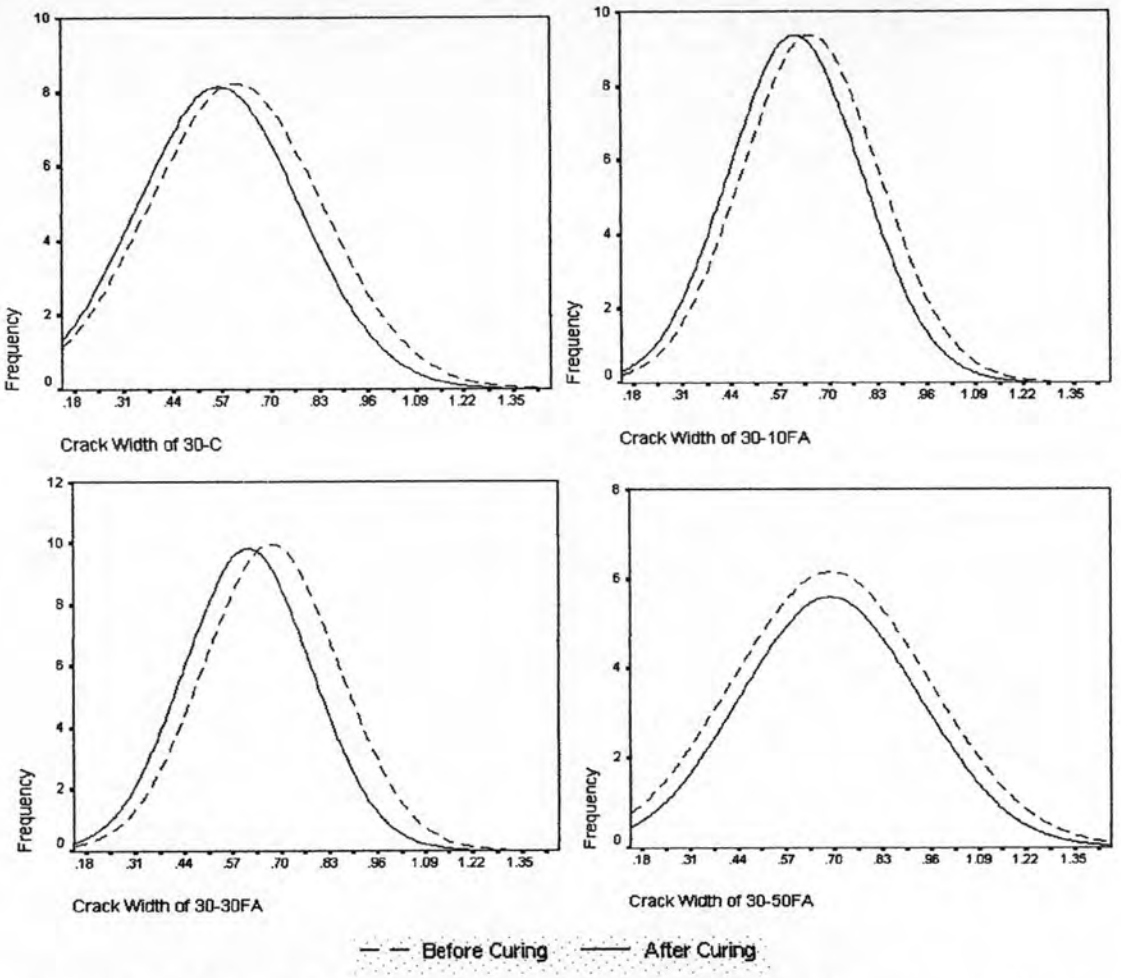

Figure 4.11: Normal distribution curve comparison for fly ash concrete specimens under air curing conditions with w/b = 0.30

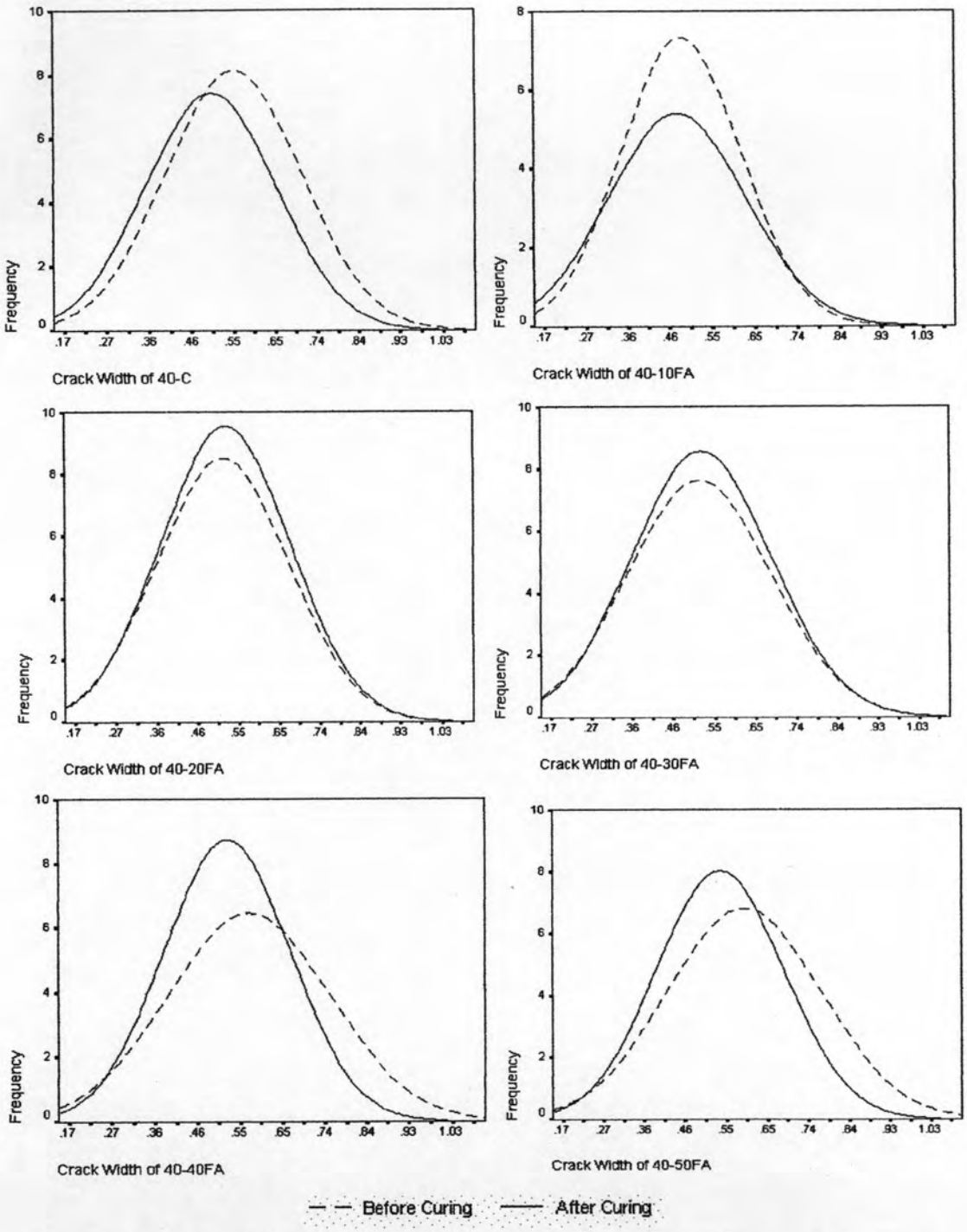

Figure 4.12: Normal distribution curve comparison for fly ash concrete specimens under air curing conditions with w/b = 0.40

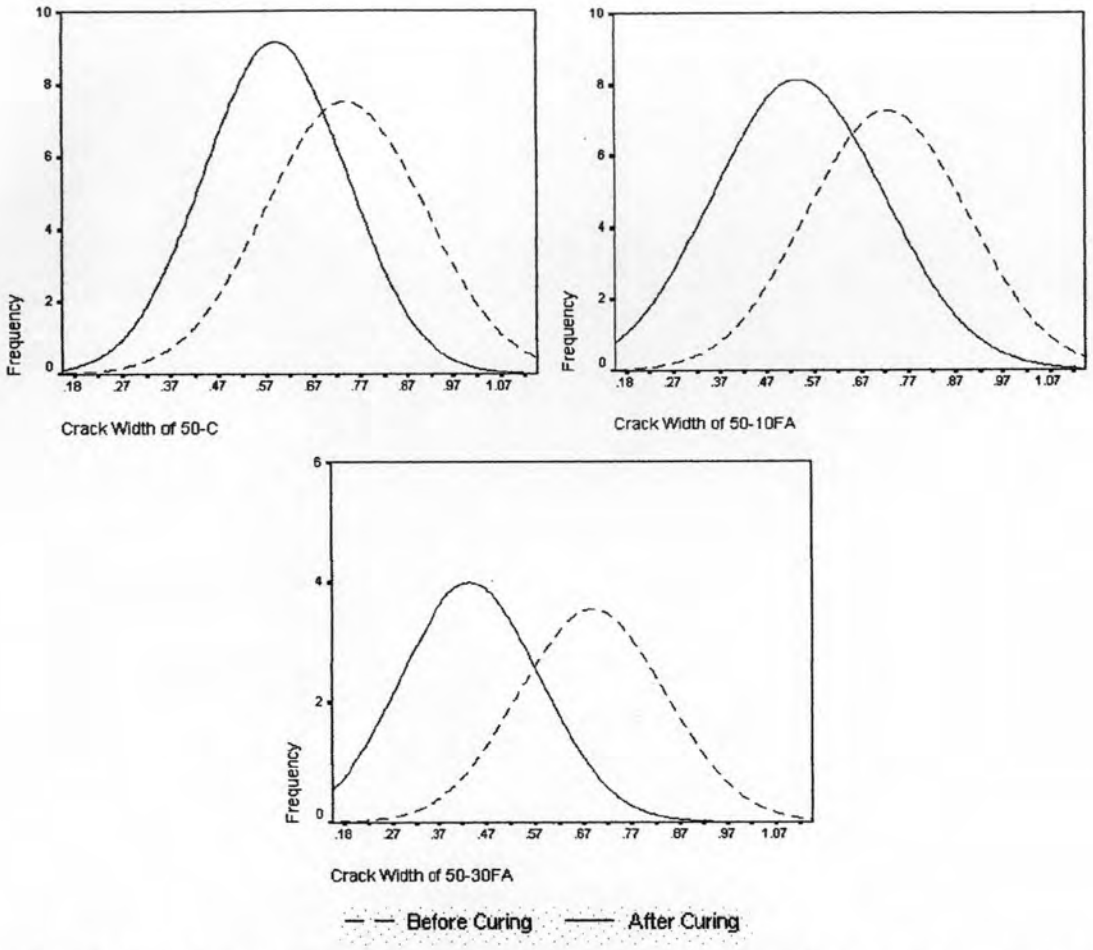

Figure 4.13: Normal distribution curve comparison for fly ash concrete specimens under air curing conditions with w/b = 0.50

For specimens with water/binder ratio of 0.50, the displacement observed (Figure 4.13) was greater than those in Figures 4.11 and 4.12 after undergoing air curing conditions. This could be due to the increase in the amount of required moisture within the concrete. Such moisture availability ensures water that would be sufficient enough for continuous hydration process. It is for this same reason that the displacement of the normal distribution curves was greater in moist cured specimens, such as in Figure 4.16, than air cured specimens.

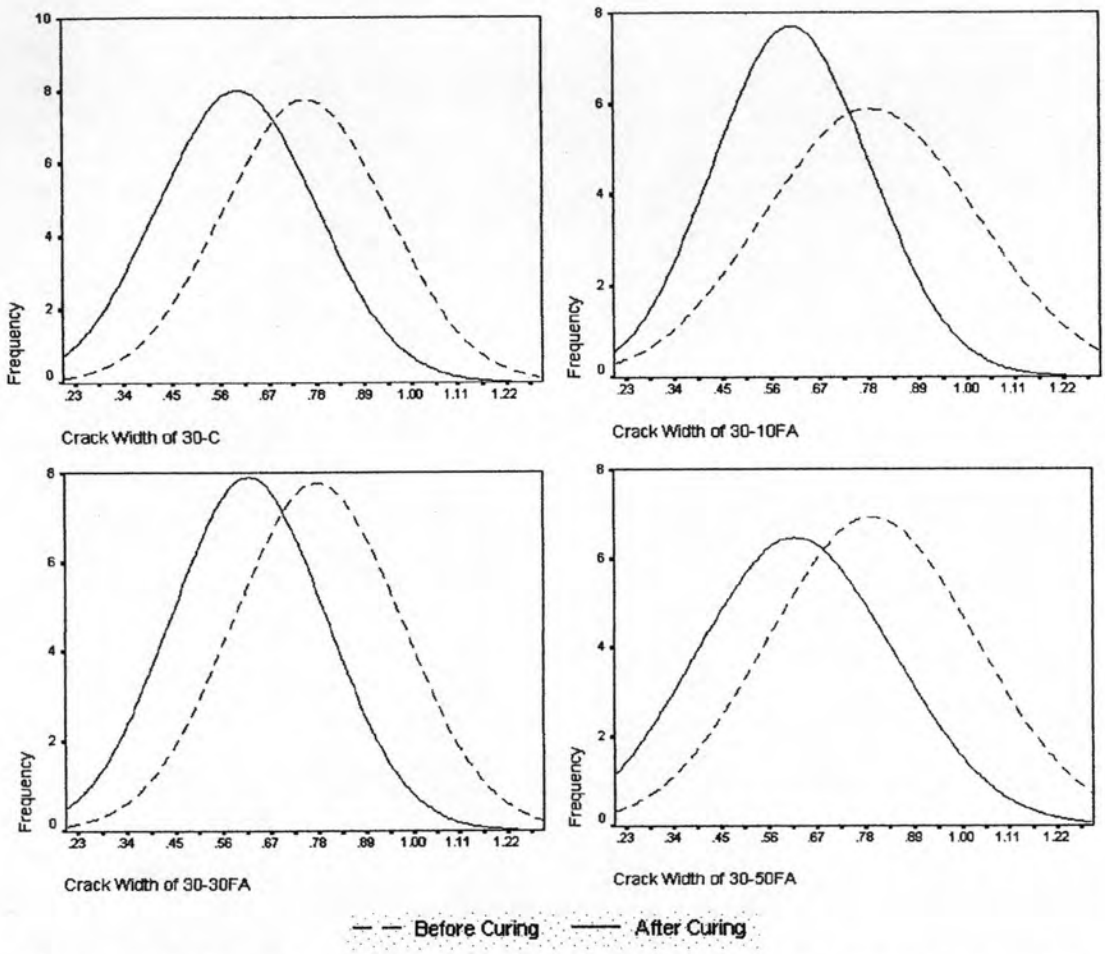

Figure 4.14: Normal distribution curve comparison for fly ash concrete specimens under moist curing conditions with w/b = 0.30

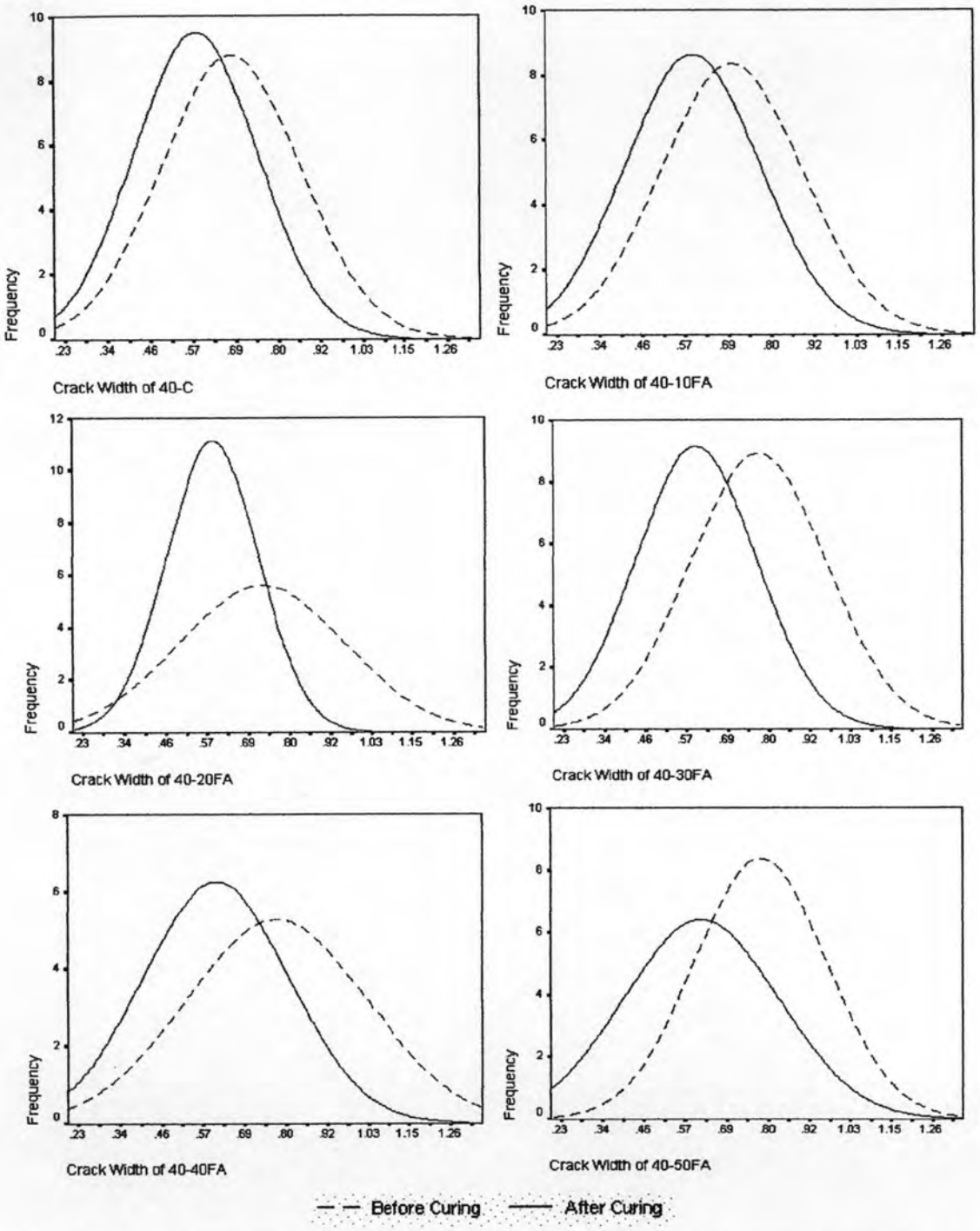

Figure 4.15: Normal distribution curve comparison for fly ash concrete specimens under moist curing conditions with w/b = 0.40

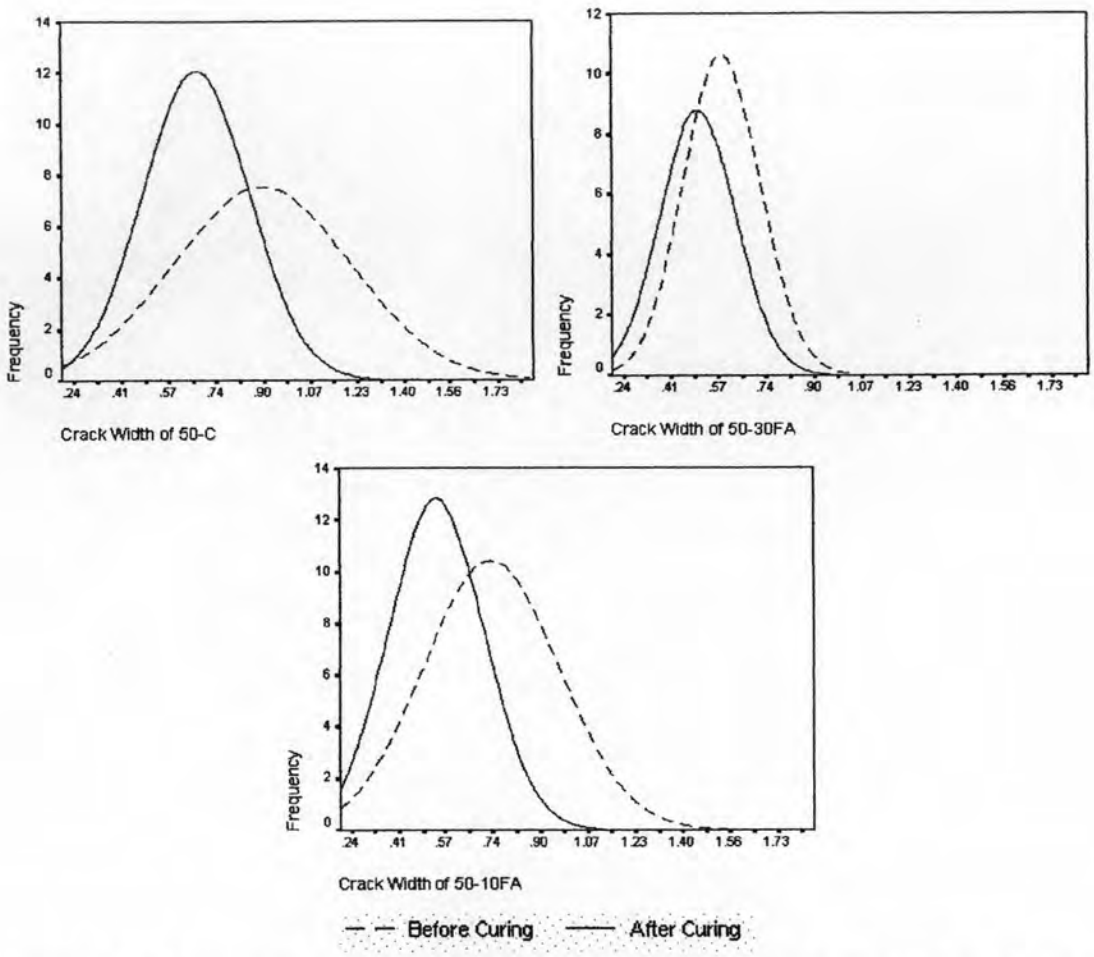

Figure 4.16: Normal distribution curve comparison for fly ash concrete specimens under moist curing conditions with w/b = 0.50

In addition to the decrease in crack width (as indicated by the displacement of the distribution curve to the left), it was observed that most of the fly ash specimens retained the shape of the distribution curve even after air curing but became narrower after moist curing. Air curing had healed the crack widths uniformly which was indicated by the shift of the curve to the left (which implied the decrease in crack width values due to healing) but still retaining the shape of the curve. This occurrence was supported by the standard deviation values in Table 4.8. The very small difference (from Day 1 to Day 28) between standard deviation values of air cured fly ash specimens implies that the shape was retained even after curing. On the other hand, moist cured specimens had decreasing standard deviation values as the amount of fly ash was used. The difference of values from the uncured state to the moist cured state indicated that the values decreased and were closer to the mean. However, the

change in normal distribution shape implied that there was a non-uniform distribution of healing by moist curing. The additional moisture from the wet burlap allowed for the production of hydration products that filled up the gaps of the plastic shrinkage cracks. However, non-uniformity of healing occurred since smaller crack widths are healed first since the gap would be easier to close or fill with hydration products than wider ones.

Table 4.8: Standard deviation values of cured fly ash concrete specimens

Designation	Standard Deviation			
	Air Curing		Moist Curing	
	Day 1	Day 28	Day 1	Day 28
30-C	0.230	0.216	0.189	0.181
30-10FA	0.182	0.177	0.238	0.177
30-30FA	0.182	0.171	0.195	0.178
30-50FA	0.265	0.241	0.238	0.224
40-C	0.154	0.148	0.188	0.166
40-10FA	0.134	0.154	0.189	0.180
40-20FA	0.154	0.151	0.232	0.128
40-30FA	0.166	0.161	0.190	0.168
40-40FA	0.182	0.141	0.252	0.202
40-50FA	0.178	0.146	0.183	0.215
50-C	0.170	0.151	0.309	0.185
50-10FA	0.170	0.181	0.236	0.166
50-30FA	0.152	0.145	0.133	0.131

From these normal distribution curves, it seemed that the percent change increases (curve moves further to the left) as the amount of fly ash increased. This was further investigated using linear regression analysis. Positive values for percent change values indicated that a decrease in crack quantification values from the uncured specimen (Day 1) to the cured specimen (Day 28) was calculated. The greater the positive calculated value to percent change would be, the greater the reduction of crack quantification values. The greater the reduction in crack quantification values, the more effective the curing condition had been in reducing plastic shrinkage cracking of concrete.

For Figures 4.17 to 4.19, the graph at the lower right corner of each figure showed the trend of the effect of fly ash content irregardless of water/binder ratio used. It represented the accumulated trend of fly ash content for water/binder ratios of

0.30, 0.40, and 0.50. As seen in Figure 4.17, there was a slight increase in percent change in average crack area as the amount of fly ash increased for specimens that were exposed to moist curing conditions. This supported the displacements seen from the normal distribution curves. On the other hand, percent change in average crack width seems to decrease the effectiveness of air curing as fly ash content increased. Similarly, both moist and air cured specimens exhibited a decrease in the percent change in maximum crack width values (Figure 4.18). This decrease may partially be due to the slow hydration process of fly ash concrete at such a period of curing time as 28 days. Regarding the percent change in crack area, Figure 4.19 has shown there was an increase in percent change as the fly ash content increased. This was attributed to the enhancement done by the curing conditions to the filling effect of fine fly ash particles.

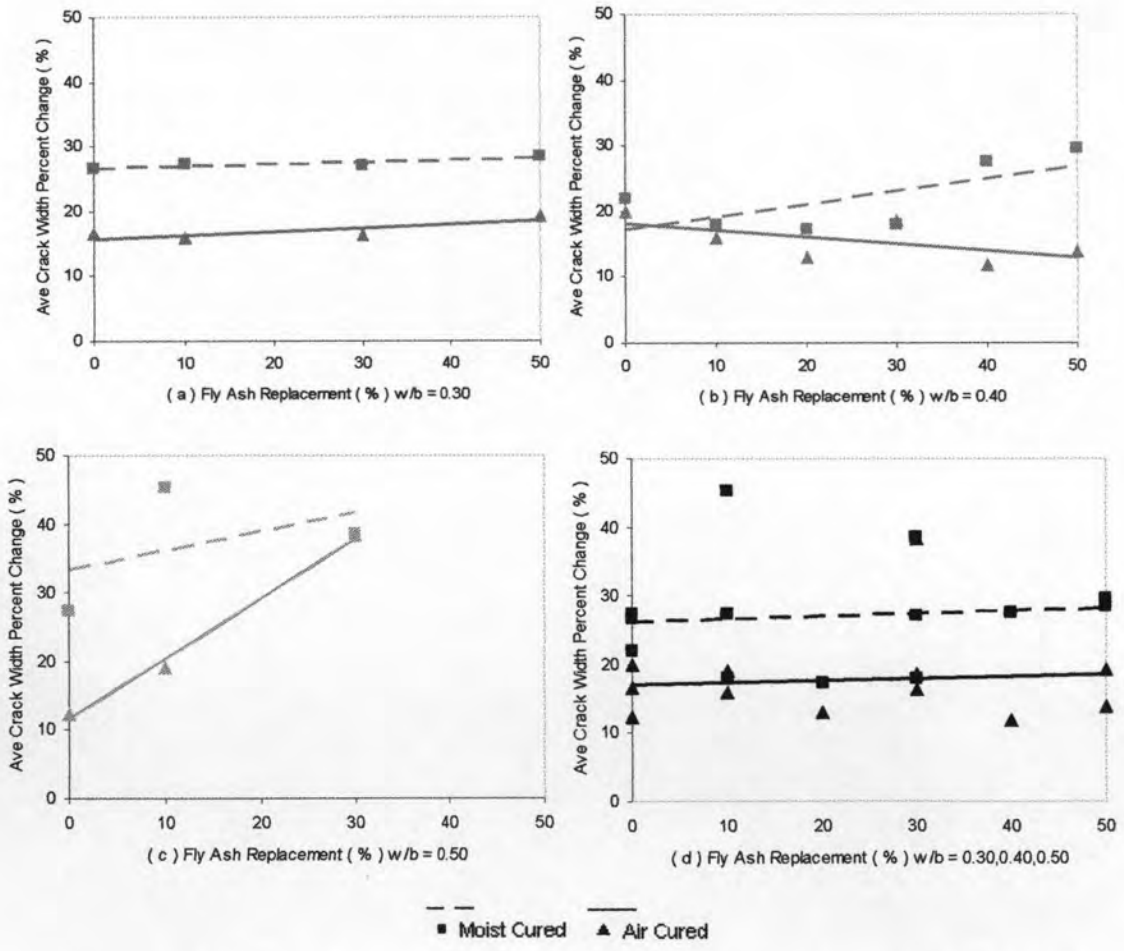

Figure 4.17: Effect of fly ash content on percent change in average crack width

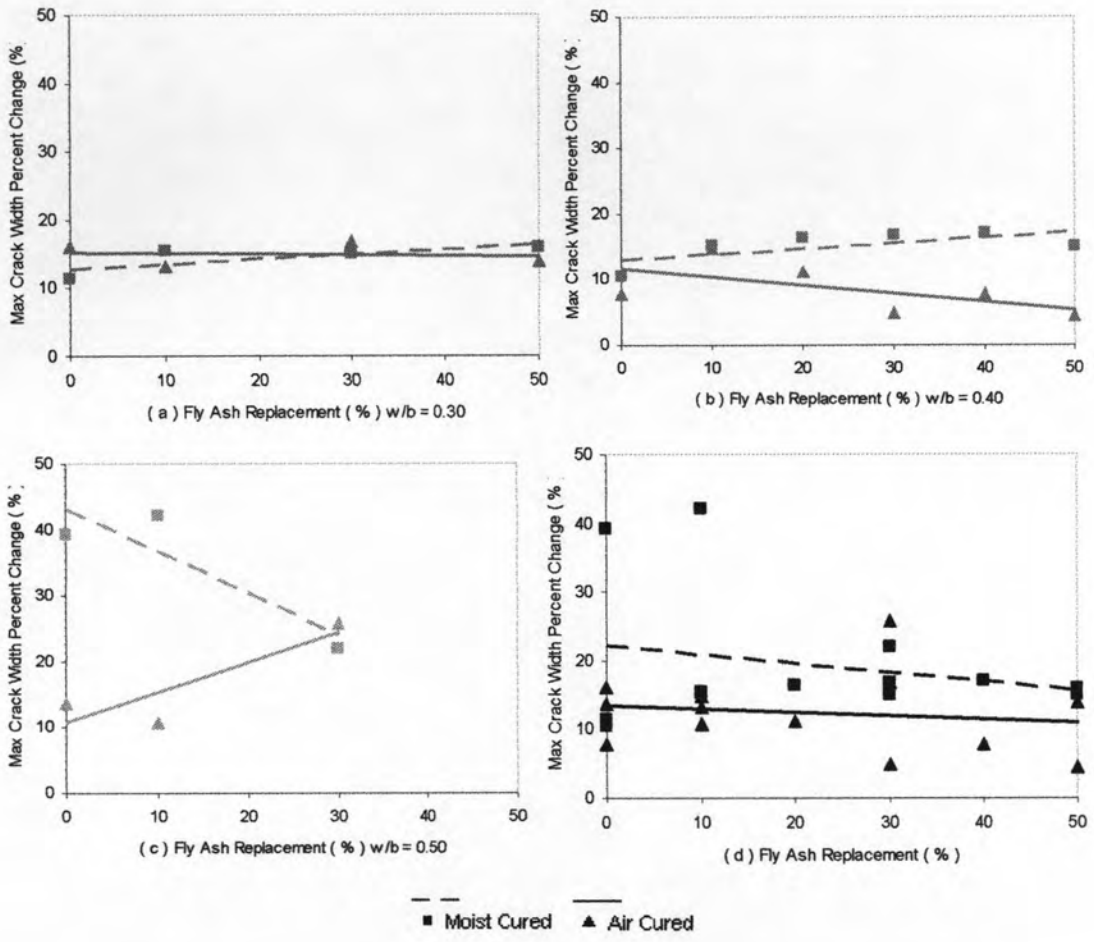

Figure 4.18: Effect of fly ash content on percent change in maximum crack width

It must be noted that Figures 4.17 to 4.19 exhibited higher percent change values for moist cured specimens than those that were exposed to air curing conditions. This clearly indicated the effectiveness of moist curing in enhancing the healing properties of concrete through enhanced hydration. Hydration was enhanced due to the sufficient amount of moisture needed for the continuous hydration process take part within the concrete matrix.

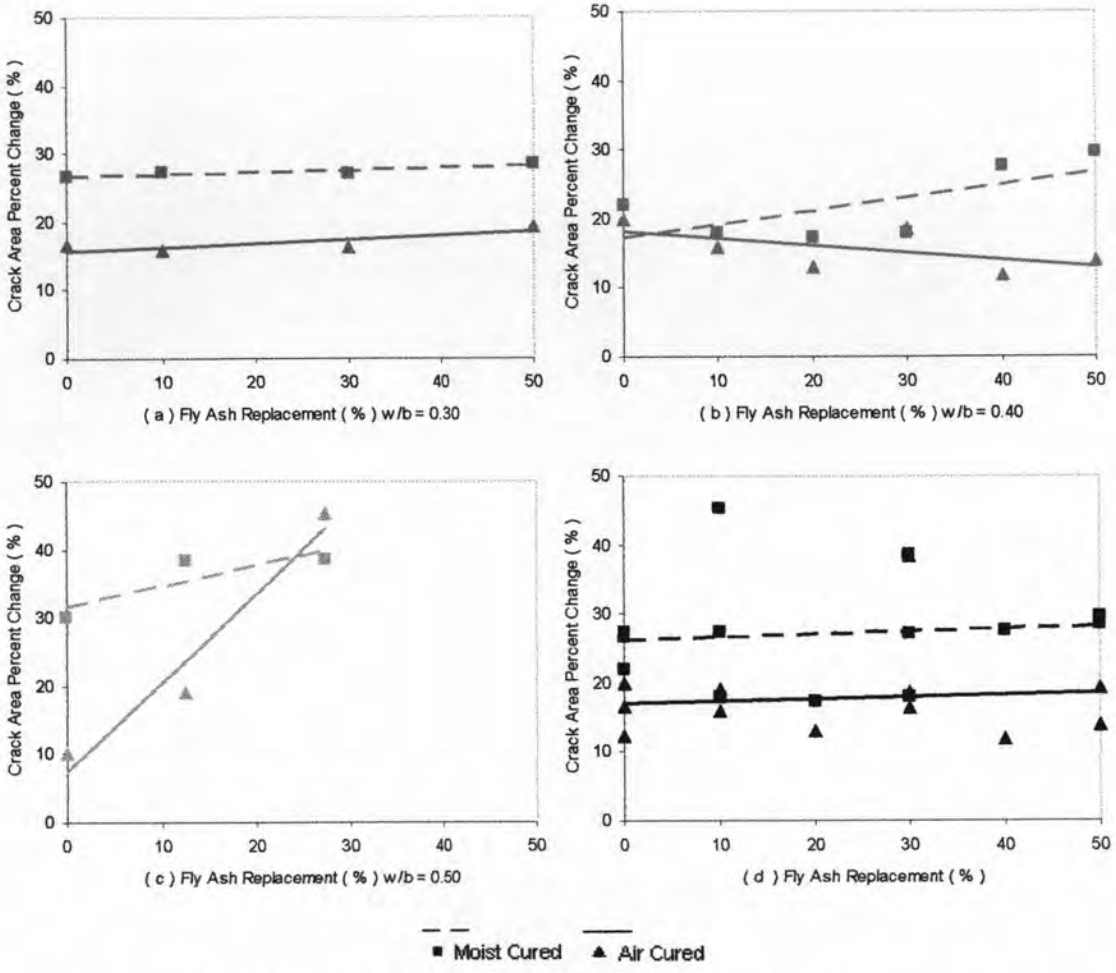

Figure 4.19: Effect of fly ash content on percent change in crack area

As in the case for the measured crack widths before curing, two approaches were used in determining the ninety percentile values of the plastic shrinkage crack widths for both air cured and moist cured specimens (as shown in Table 4.9). Once again, it was observed that these values were greater than the tolerable crack width values in ACI 224R. In addition to this, the mean crack width values of either the moist cured or air cured specimens (Table 4.10) also exceeded ACI 224R tolerable crack width values. Although exposure to curing for 28 days had reduced the plastic shrinkage crack widths of fly ash concrete, additional measures appears to be needed in order to further reduce possible permeability problems caused by plastic shrinkage cracks when the same mix proportion is used with under similar environmental conditions and sufficient restraints.

Table 4.9: Ninety percentile crack width values of chosen fly ash concrete specimens after curing

Designation	90 Percentile Crack Width							
	Air Curing				Moist Curing			
	Day 1		Day 28		Day 1		Day 28	
	Normal	Sort	Normal	Sort	Normal	Sort	Normal	Sort
w/b-%FA	mm	mm	mm	mm	mm	mm	mm	mm
30-C	0.91	0.90	0.85	0.85	1.02	1.02	0.82	0.82
30-10FA	0.91	0.85	0.94	0.86	1.08	1.08	0.82	0.79
30-30FA	0.95	0.90	0.87	0.79	1.02	1.02	0.87	0.83
30-50FA	1.02	0.98	1.02	0.99	1.13	1.11	1.00	0.94
40-C	0.77	0.74	0.67	0.67	0.93	0.93	0.79	0.79
40-10FA	0.67	0.66	0.66	0.64	0.99	0.95	0.85	0.80
40-20FA	0.75	0.74	0.73	0.67	0.98	0.94	0.75	0.75
40-30FA	0.78	0.77	0.73	0.68	1.05	1.04	0.85	0.80
40-40FA	0.79	0.79	0.67	0.67	1.09	1.04	0.92	0.91
40-50FA	0.86	0.84	0.68	0.68	1.04	1.04	0.99	0.94
50-C	0.96	0.96	0.77	0.77	1.35	1.29	0.92	0.92
50-10FA	0.97	0.96	0.77	0.73	1.08	1.02	0.74	0.73
50-30FA	0.95	0.85	0.69	0.63	0.79	0.67	0.68	0.63

Table 4.10: Mean crack widths of chosen fly ash concrete specimens after curing

Designation	Mean Crack Width			
	Air Curing		Moist Curing	
	Day 1	Day 28	Day 1	Day 28
w/b-%FA	mm	mm	mm	mm
30-C	0.611	0.565	0.753	0.597
30-10FA	0.655	0.614	0.782	0.605
30-30FA	0.676	0.613	0.775	0.617
30-50FA	0.692	0.690	0.792	0.617
40-C	0.555	0.504	0.676	0.582
40-10FA	0.484	0.474	0.698	0.594
40-20FA	0.516	0.522	0.726	0.588
40-30FA	0.519	0.523	0.775	0.600
40-40FA	0.573	0.524	0.777	0.609
40-50FA	0.594	0.539	0.783	0.618
50-C	0.744	0.596	0.897	0.668
50-10FA	0.731	0.524	0.730	0.539
50-30FA	0.694	0.440	0.584	0.501

Weekly observations were done in order to check the effectiveness of curing, whether air curing (Figures 4.20-4.22) or moist curing (Figures 4.23-4.25). From the graphs generated from the crack quantification values calculated on a weekly basis, it was observed that most of the decrease in values for average crack width (Figures

4.20 and 4.23), maximum crack width (Figures 4.21 and 4.24) and crack area (Figures 4.22 and 4.25) occurred after seven days (or one week) exposure to either curing conditions. This is indicated by the relatively steeper slope observed after the first week as compared to the other generated slopes from the following weeks. This would mean that fly ash specimens cured for at least seven days to be able to obtain a substantial amount of decrease in crack quantification values. Note that week 0 corresponded to the quantified crack values at the end of plastic shrinkage cracking test at final setting time.

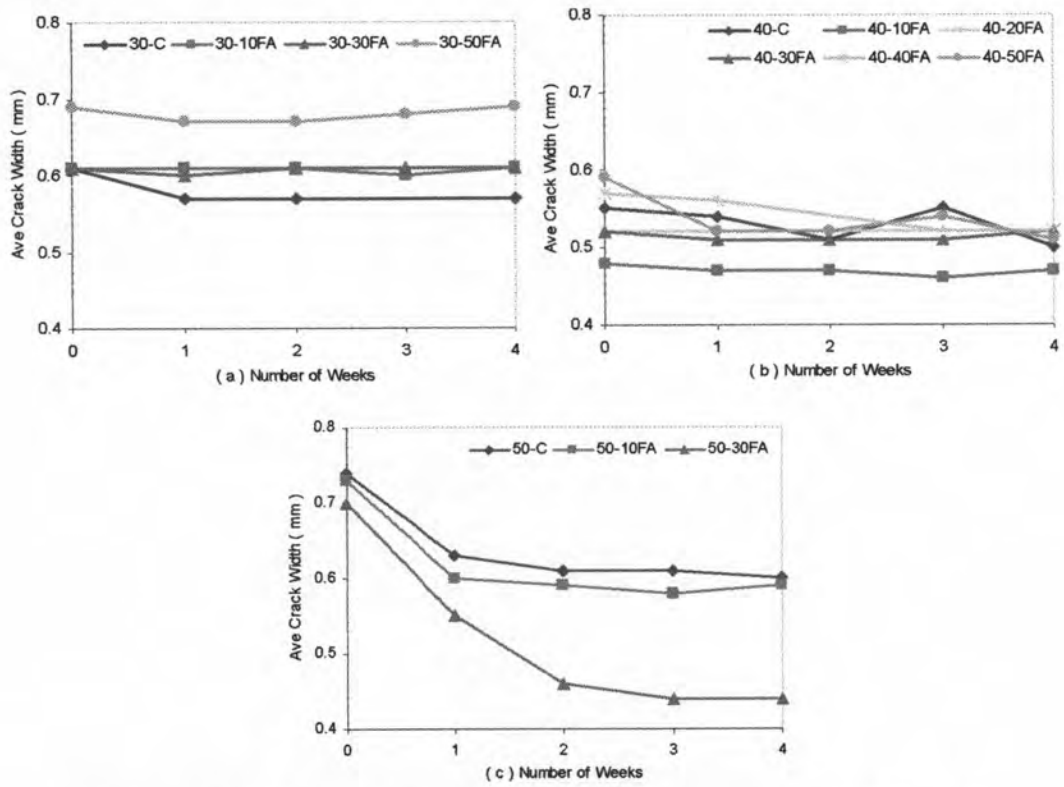

Figure 4.20: Effect of duration of air curing on average crack width of fly ash concrete specimens

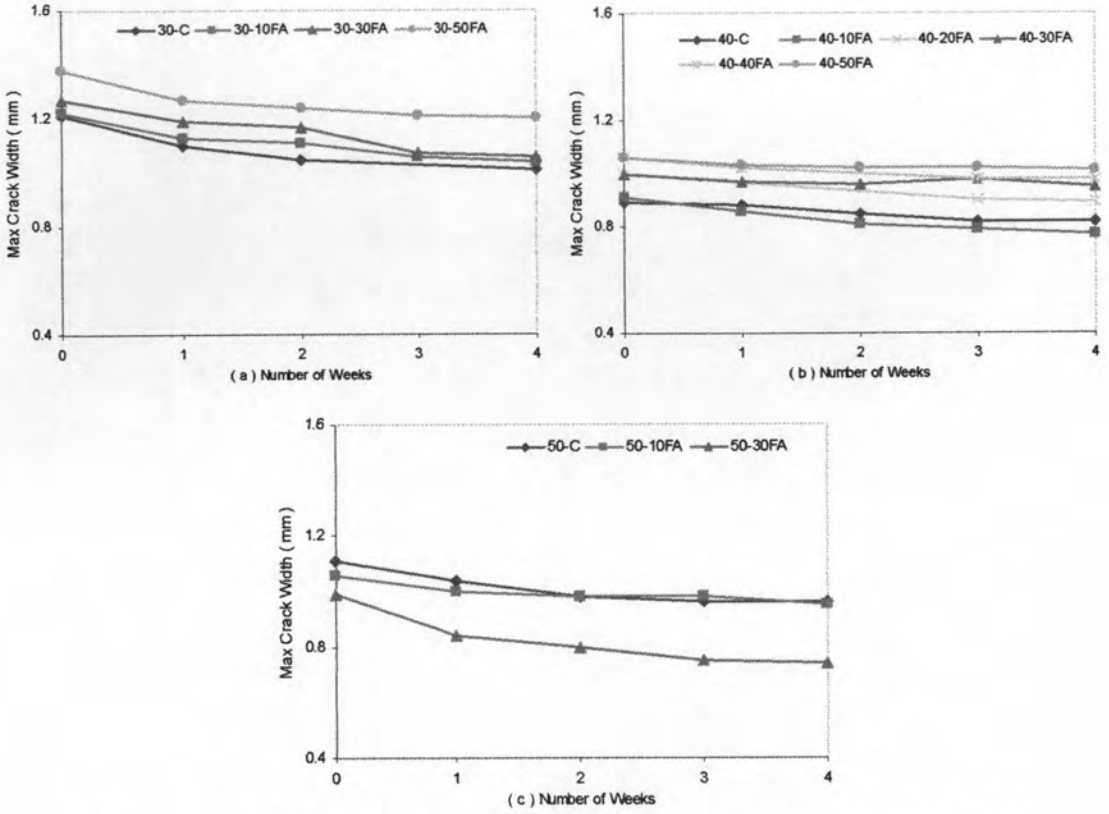

Figure 4.21: Effect of duration of air curing on maximum crack width of fly ash concrete specimens

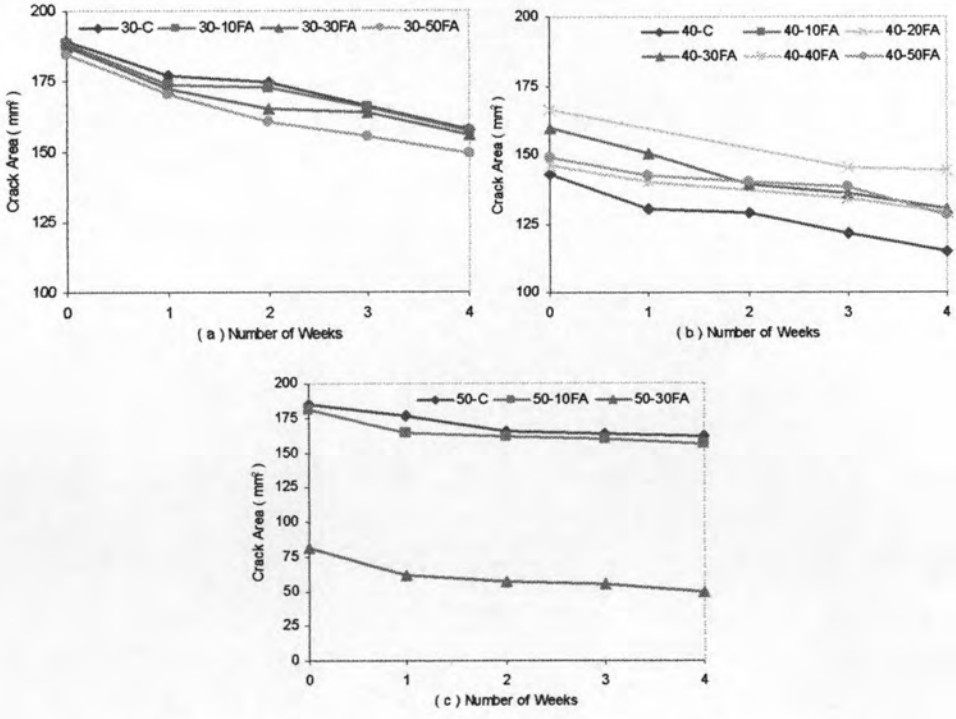

Figure 4.22: Effect of duration of air curing on crack area of fly ash concrete specimens

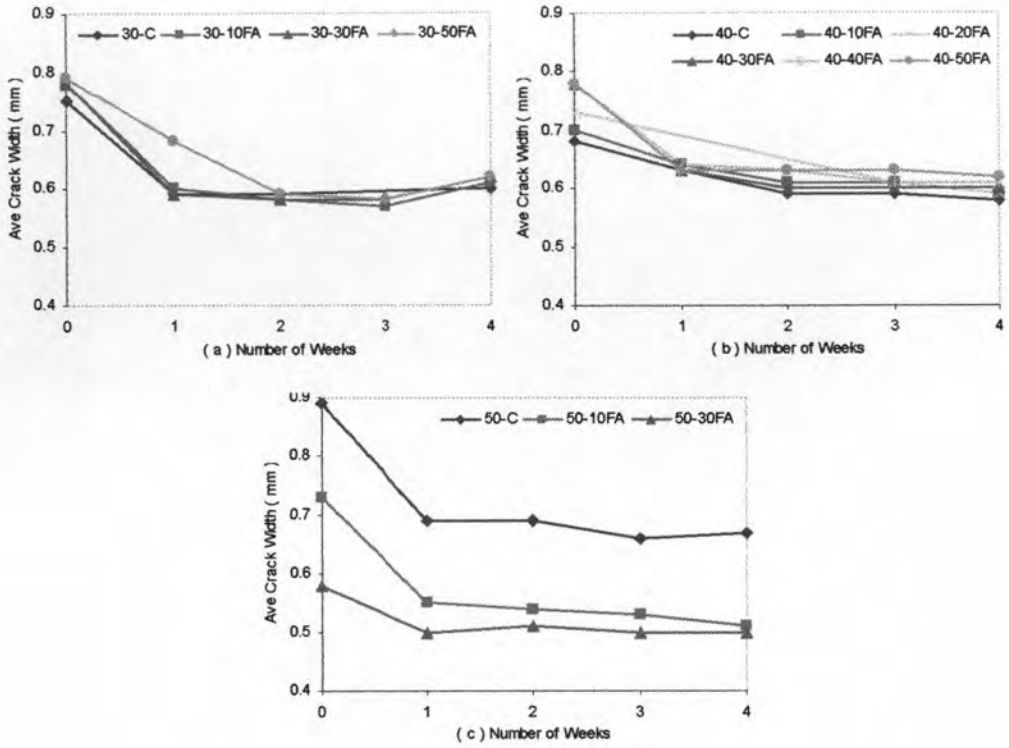

Figure 4.23: Effect of duration of moist curing on average crack width of fly ash concrete specimens

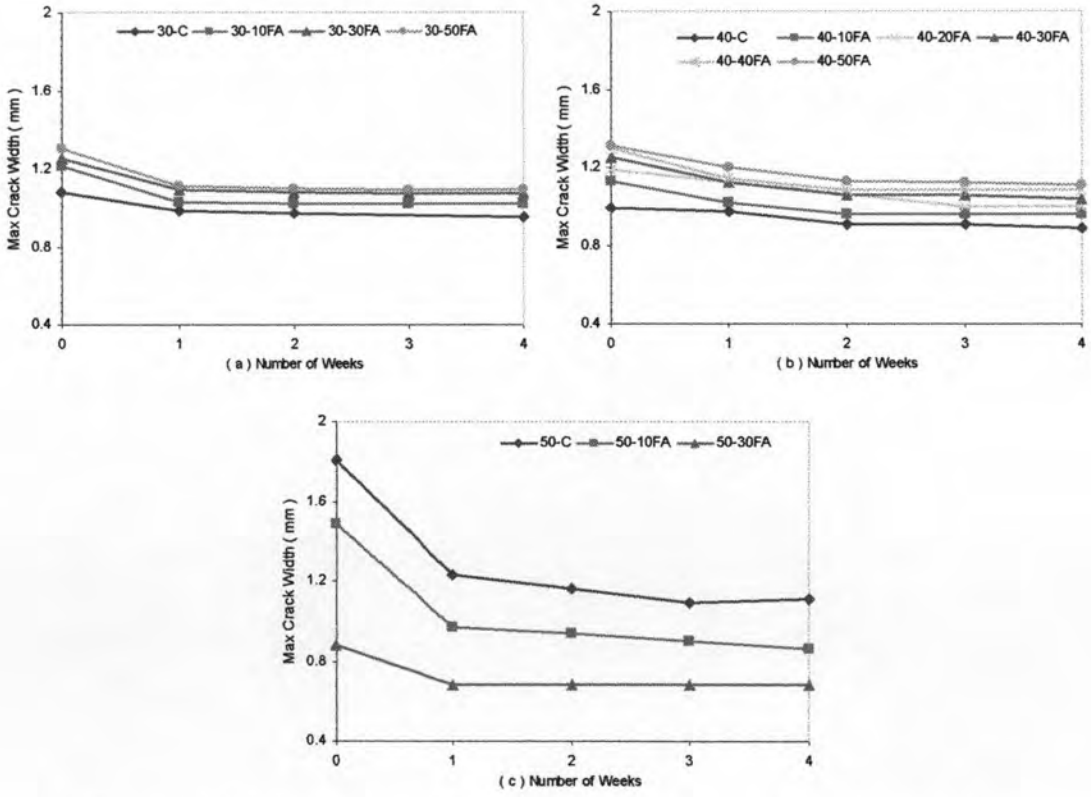

Figure 4.24: Effect of duration of moist curing on maximum crack width of fly ash concrete specimens

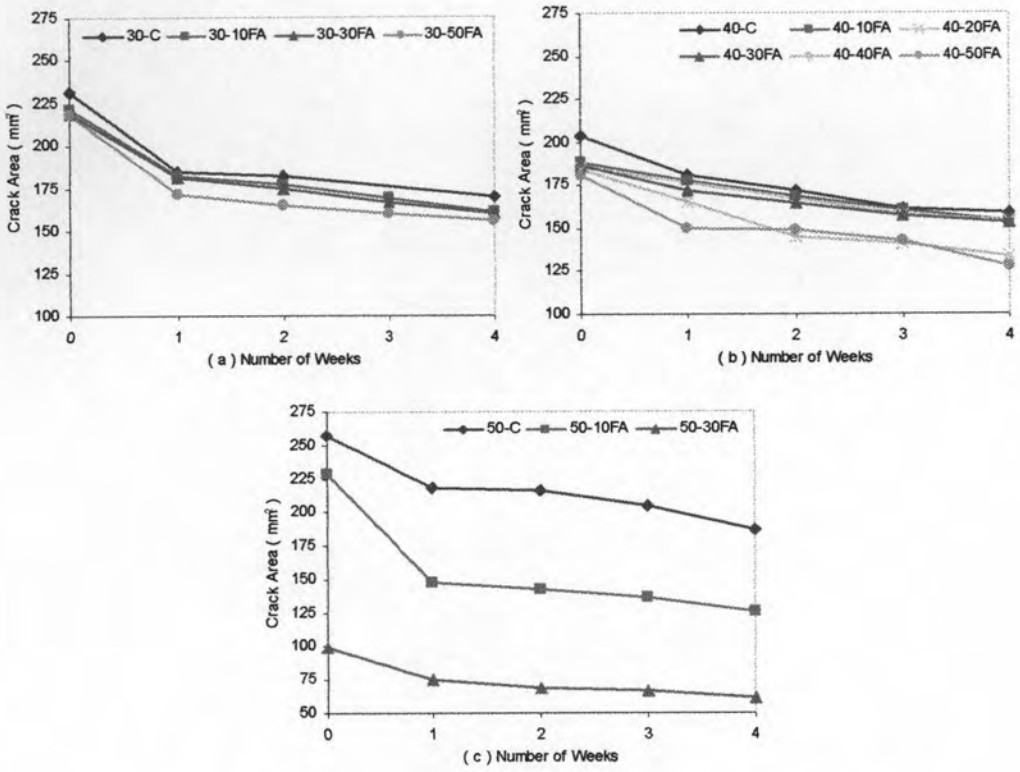

Figure 4.25: Effect of duration of moist curing on crack area of fly ash concrete specimens

4.1.6 Cracking Reduction Ratio of Fly Ash Concrete

As suggested by ASTM 1579-06, the effectiveness of pozzolan used with respect to the use of plain ordinary Portland cement would be determined by the calculated values of the cracking reduction ratio (using the Formula 3.6 in Chapter III). Positive values of the calculated cracking reduction ratio would show the effectiveness of fly ash against plain ordinary Portland cement to reduce plastic shrinkage crack widths in concrete.

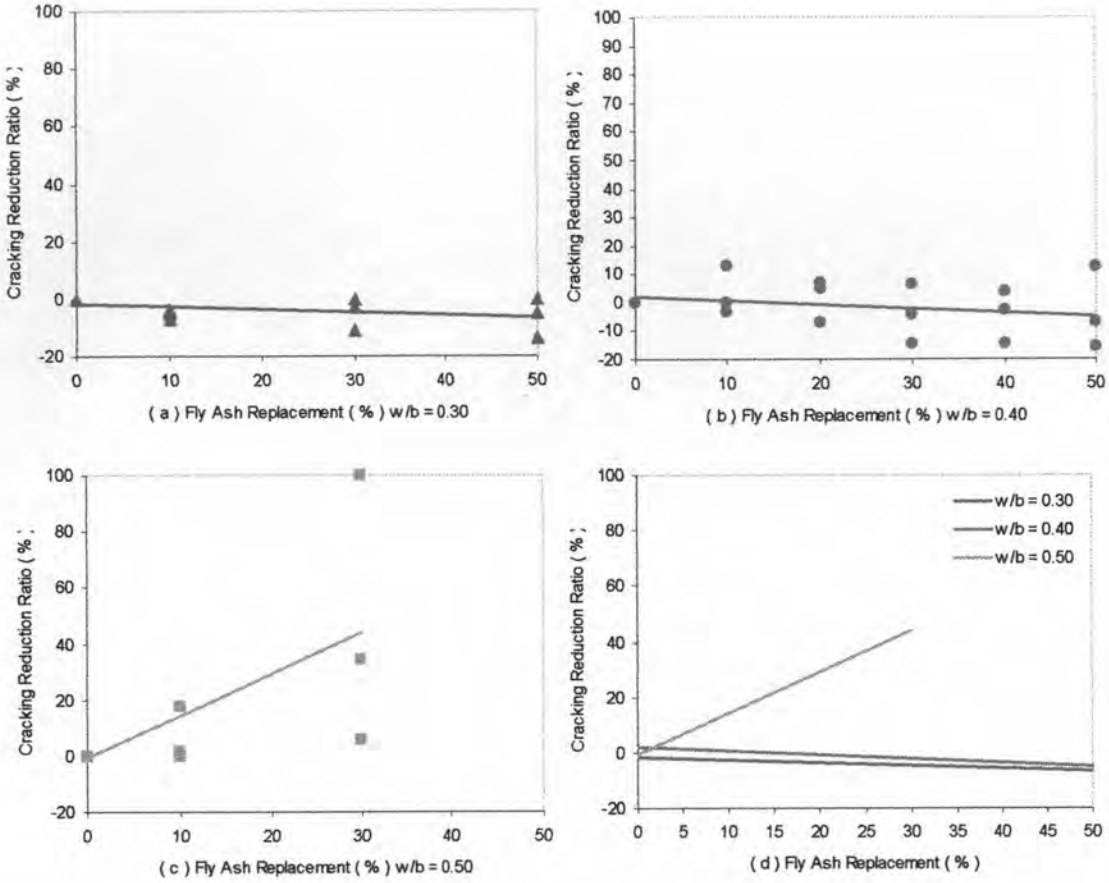

Figure 4.26: Effect of fly ash content on cracking reduction ratio

From Figure 4.26, it seems that the values for cracking reduction ratio of specimens with water/binder ratio of 0.30 were decreased even as the amount of fly ash was increased. This result was in accordance with the corresponding increase in crack width as well as the slight decrease in crack area. Such behavior indicated that the use of fly ash with water/binder ratio of 0.30 would not be effective enough to reduce plastic shrinkage cracks as compared to using plain ordinary Portland cement.

For specimens with water/binder ratio of 0.40, increasing the amount of fly ash used in concrete also decreases the effectiveness of fly ash to reduce plastic shrinkage cracks. However, it is interesting to note that from these observations fly ash replacement of 10 to 15 percent was seen as more effective in reducing plastic shrinkage cracks than the control specimen. Replacement of cement by fly ash greater than 15%, based on generated trend from experimental observation, would call for caution as to the possible occurrence of increase in plastic shrinkage cracks.

The increasing slope of the cracking reduction ratio values for specimens with water/binder ratio of 0.50 pointed out that the effectiveness of fly ash to reduce plastic shrinkage cracks increased as the amount of fly ash increased. Nevertheless, it must be noted that the increase in effectiveness in plastic shrinkage crack reduction with the increasing amount of fly ash content in concrete with water/binder ratio of 0.50 has a corresponding decrease in compressive strength (as previously presented in the properties in Table 4.1). Thus, the use of fly ash replacement of 10 to 15% with water/binder ratio of 0.40 would effectively reduce plastic shrinkage cracks without compromising compressive strength.

In addition to this, care must still be exercised in using fly ash as a means to control plastic shrinkage cracking. Even as the use of fly ash could reduce plastic shrinkage cracking and with aid of curing procedures could further reduce such cracks, further measures would still be needed to ensure that the crack widths would be able to withstand different exposure conditions as suggested by the tolerable crack width values of ACI 224R. For this purpose, invulnerability to dry air exposure conditions could be possible by further increasing fly ash content with water/binder ratio of 0.50 and proper curing procedures. However, using such mix proportions compromises compressive strength at early ages.

4.1.7. Summary of Results of Fly Ash Concrete

Figures 4.21 to 4.23 summarize the tendency of the influence of the amount of fly ash on plastic shrinkage cracking. For specimens with water/binder ratio of 0.30 (Figure 4.27), the average crack width and maximum crack width tend to increase as the amount of fly ash increased. However, crack area has a tendency to slightly decrease as fly ash content increased. Also, the cracking reduction ratio was seen to decrease as the amount of fly ash increased. Specimens using water/binder ratio of 0.40 (Figure 4.28) behaved similarly as specimens with water/binder ratio of 0.30 as the amount of fly ash increased. Specimens using 0.50 water/binder ratio (Figure 4.29) performed otherwise as the average crack width, maximum crack width and

crack area decreased as the fly ash content increased. In addition to this, the cracking reduction ratio increased with the amount of fly ash used.

It was also observed that plastic shrinkage cracks, in terms of average crack width, maximum crack width, crack area, and cracking reduction ratio, were further reduced by using moist curing by wet burlap for 28 days. The percent change in reduction of these values was greater in moist cured specimens than air cured specimens.

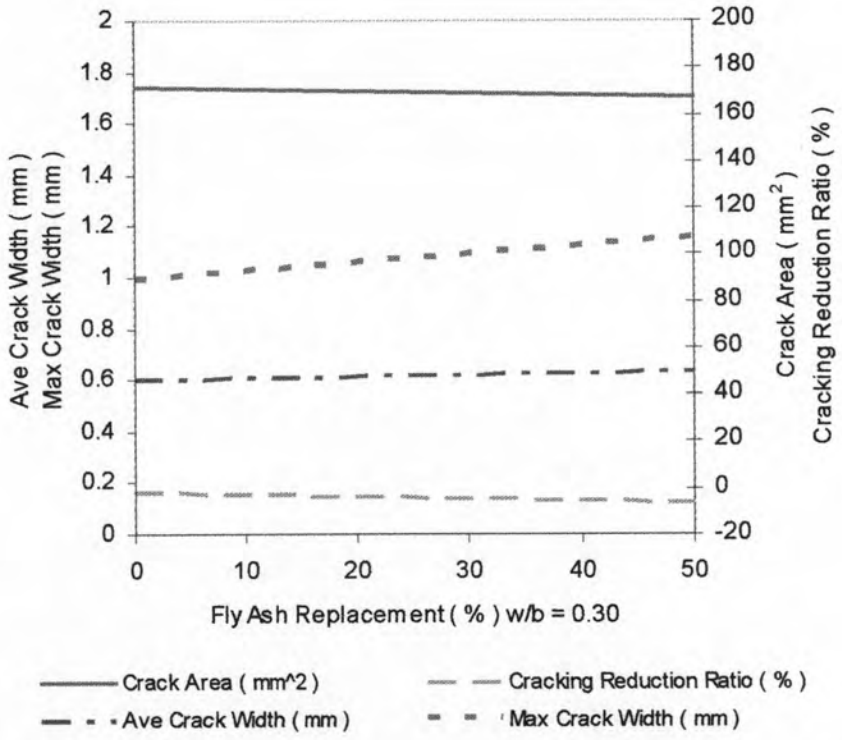

Figure 4.27: Effect of fly ash content on average crack width, maximum crack width, crack area, and cracking reduction ratio with w/b = 0.30

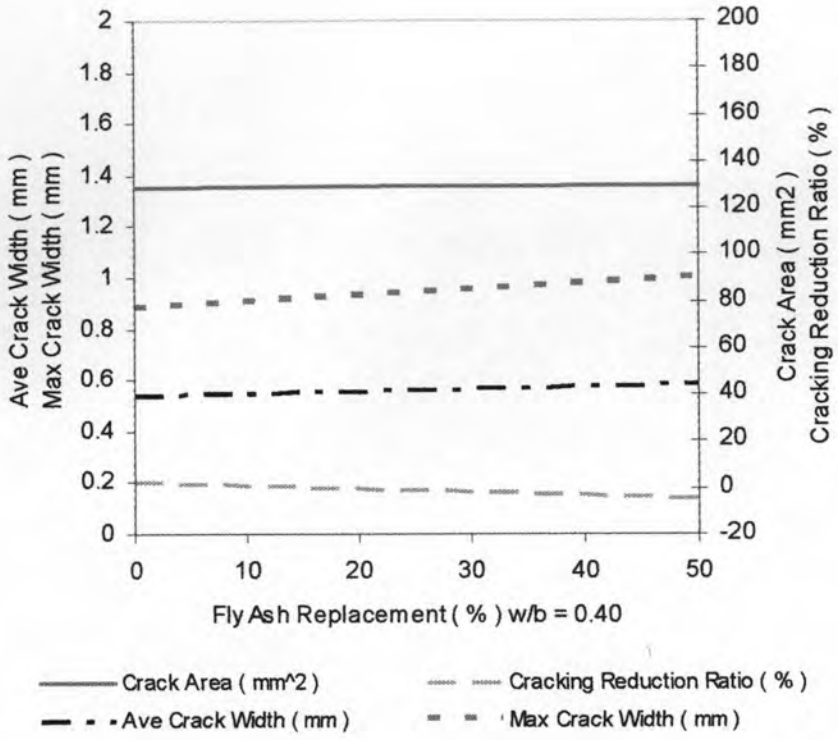

Figure 4.28: Effect of fly ash content on average crack width, maximum crack width, crack area, and cracking reduction ratio using water/binder ratio = 0.40

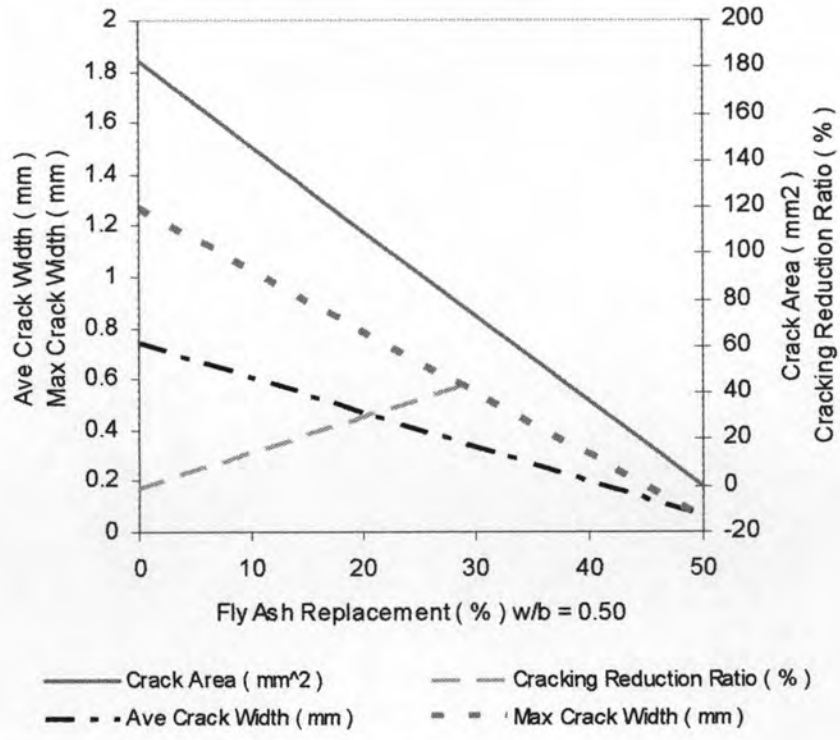

Figure 4.29: Effect of fly ash content on average crack width, maximum crack width, crack area, and cracking reduction ratio using water/binder ratio = 0.50

4.2. Effect of Silica Fume on Plastic Shrinkage Cracking of Concrete

4.2.1 Properties

Table 4.11 lists the properties of silica fume concrete. The concrete mix became less workable as the amount of silica fume was increased. The slump recorded decreased as the silica fume content increased. Such behavior was due to the introduction of large surface area of the silica fume particles in the concrete mix.

Increasing the amount of silica fume decreased the setting time. Such decrease may be attributed to the increase in cohesion from the increase in water demand. It was also observed that there was little to no bleeding when silica fume concrete was mixed. This was caused by the high surface area of the silica fume to be wetted and therefore reducing the amount of free water left in the mix for bleeding. Silica fume reduced bleeding by physically blocking the pores in the fresh concrete (decreasing the amount of bleed channels) which also led to the slow movement of free water (if any) from the interior to the concrete surface. Since bleeding was low, it was essential to finish the concrete as soon as it was placed and compacted. The silica fume concrete, being more cohesive and exhibited little to no bleeding, made the concrete more difficult to place in the panel formworks.

Table 4.11: Properties of silica fume concrete

Designation	w/b ratio	Silica Fume Used	Time of Setting		Slump	Compressive Strength (28-day)
			Initial	Final		
w/b-%SF	w/b	%SF	hr:min	hr:min	cm	ksc
50-C	0.50	0	3:29	4:38	13.3	335
50-3SF		3	3:10	4:35	8.2	335
50-5SF		5	2:57	4:17	5.3	348

C = Control Specimen SF = Silica Fume w/b = Water/Binder Ratio

As seen in Table 4.11, the compressive strength after 28 days increased as the amount of silica fume content increased. Generally, compressive strength of silica fume concrete would be higher than control specimens due to the pozzolanic reaction that occurs as a result of using silica fume in the concrete mix.

The appearance of the first crack in the silica fume mixes could be seen in Table 4.12. Despite the increase in stiffness (as compared to 50-C mixes), it took some time for the initial crack to appear. The recorded evaporation rate and environmental conditions (wind velocity, temperature, and relative humidity) taken as the average values throughout the whole testing duration as shown in Table 4.12.

Table 4.12: Time of appearance of first crack in silica fume concrete specimens

Designation	Time of Crack Appearance	Evaporation Rate	Wind Velocity	Temperature	Relative Humidity
w/b-%SF	min	min	m/s	°C	%
50-C	90	1.06	4.0	36.5	46
50-3SF	90	1.09	4.0	35	30
50-5SF	90	1.08	4.0	35	31

4.2.2 Effect on Average Crack Width

Histogram plots of silica fume specimen crack widths (from all three specimens per silica fume concrete mix) were shown in Figure 4.30. It could be seen in the statistical parameters in Table 4.13 that the calculated means and medians were similar which implied that the distribution would be symmetrical. As in the case of the fly ash concrete specimens, the value of the mode would not be determined from the generated histogram as it was determined from the recorded measured widths with the most number of occurrences (per single measured value) and the histogram shows the accumulated frequencies per range. Once again, the mode was lesser than the mean. In other words, the most occurring crack width would be lesser than the average measured crack width. It was observed that the mode values of the measured crack widths from the silica fume concrete specimens seem to be lesser than the mode values of the fly ash concrete specimens. This could imply that the use of silica fume as replacement for cement could generate narrower crack widths than the use of fly ash in concrete. It was determined that the variation of the measured crack widths were very small as proven by the variance values from the same table. Normal distribution curves of silica fume specimens were analyzed as shown in Figure 4.31. It could be clearly seen that the curve was displaced to the left, with respect to the peak

of the normal distribution curve of the control specimen. As the amount of silica fume increased, the further the displacement was to the left of the control specimen. This indicated that increasing the amount of silica fume content in concrete would have a corresponding decrease in average crack width. However, such decrease was not quite enough as the mean crack width values of the silica fume concrete specimens were larger than the tolerable crack widths as suggested by ACI 224R (Table 4.5).

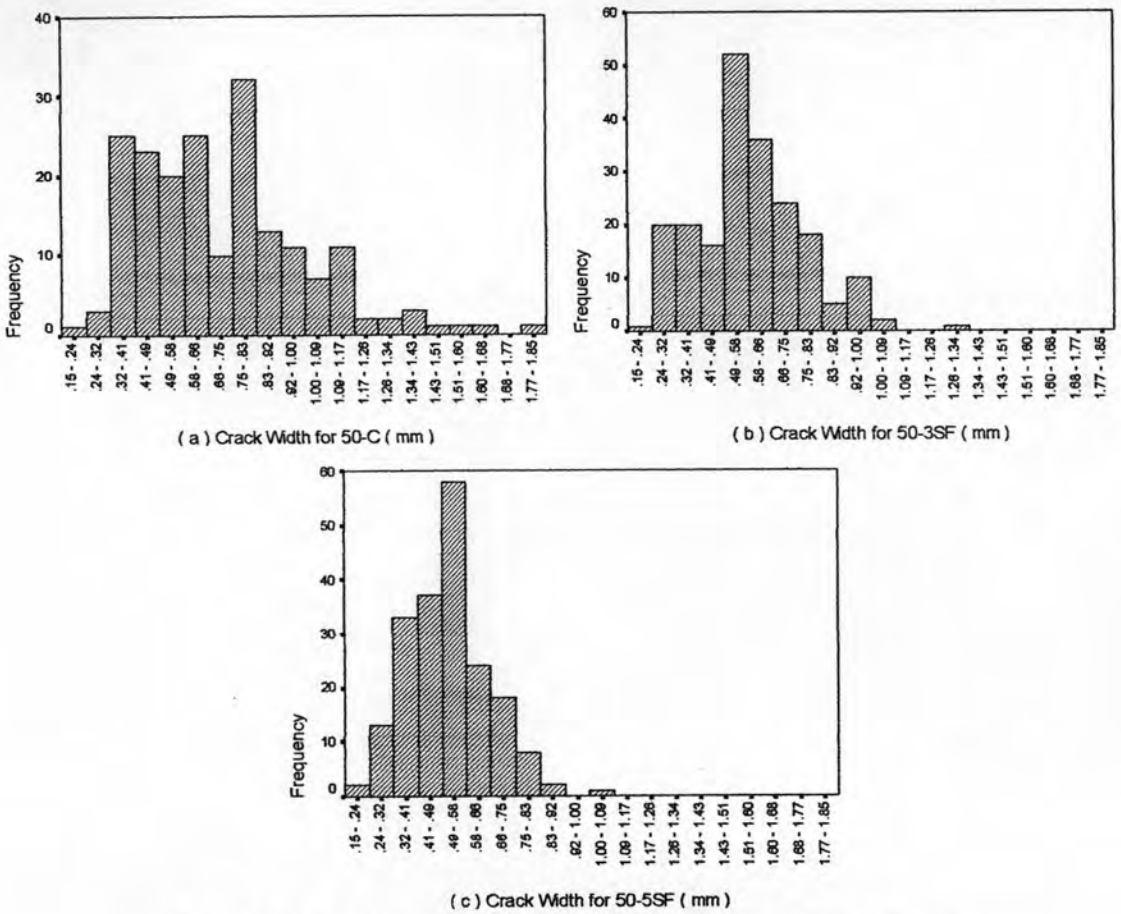

Figure 4.30: Histogram plots of crack widths of silica fume concrete specimens

Table 4.13: Statistical parameters of silica fume concrete crack widths

Designation	Data Points	Mean	Median	Mode	Variance	Standard Deviation
w/b-%SF	-	mm	mm	mm	mm	mm
50-C	192	0.708	0.640	0.77	0.084	0.289
50-3SF	205	0.577	0.570	0.54	0.034	0.186
50-5SF	196	0.508	0.490	0.43	0.019	0.139

As seen in Table 4.13, the standard deviation values decreased as the silica fume content increased. This created narrower distribution curves (Figure 4.31) which also indicated that as the amount of silica fume in concrete increased, plastic shrinkage crack widths tend to be more uniform and closer to the calculated mean value.

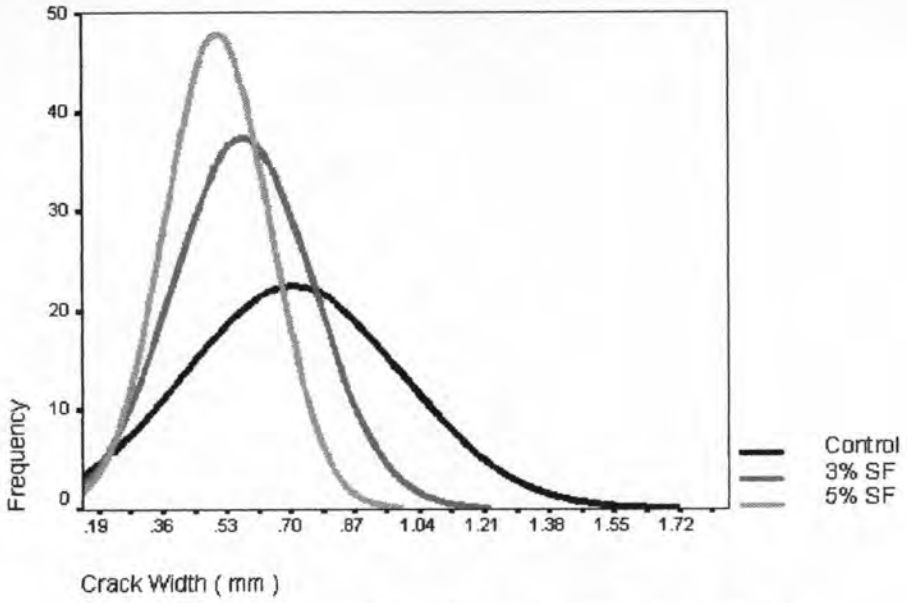

Figure 4.31: Normal distribution curve of crack width of silica fume concrete specimens

As in the case of fly ash concrete, linear regression analysis of the calculated average crack widths was done in order to support such findings from Figure 4.31. Linear regression was chosen once again due to the relatively higher significance it generates as compared to other statistical models. From linear regression, the trends or tendencies of silica fume behavior with respect to plastic shrinkage cracking would be further determined.

It could be clearly seen in Figure 4.32 that increasing the amount of silica fume in concrete would result in a corresponding decrease in the average crack widths. This supported the observed behavior of the displacements of the normal distribution curves as the silica fume content increased. The decrease in the average crack width values was attributed to the micro filler effect of the dispersed silica fume in the concrete matrix. ACI 234R (Guide for the Use of Silica Fume in Concrete)

estimates that for a 15 percent silica fume replacement of cement, there are approximately 2,000,000 particles of silica fume for each rain of Portland cement. Since silica fume particles are known to be approximately $1/50^{th}$ the size of an average Portland cement particle (0.10 to 0.30 μm), silica fume particles could easily fill up voids that cement particles could not. This is also why it is imperative that the silica fume pellets used in this research must be dry mixed with aggregates first. In order to fully take advantage of the micro filler effect of the ultrafine particles of silica fume, the silica fume pellets must undergo such grinding process.

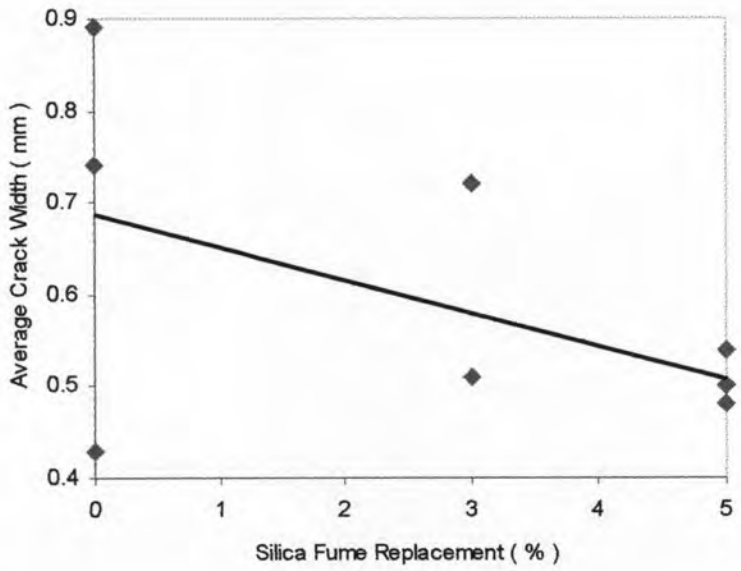

Figure 4.32: Effect of silica fume content on average crack width

4.2.3 Effect on Maximum Crack Width

Once again, the micro filler effect of silica fume particles influenced the trend of maximum crack width in silica fume concrete. Similar to the behavior of the calculated average crack width, the maximum crack width decreased as the amount of silica fume used in the concrete was increased (Figure 4.33). Such behavior adds to the ability of silica fume to reduce plastic shrinkage cracking of concrete which would inevitably improve the penetrability of concrete. The combination of high reactivity and extreme fineness would results in the possibility of producing more dense concrete with very low porosity. Since the pores would be small and discontinuous then it would also lead to high strength and low penetrability.

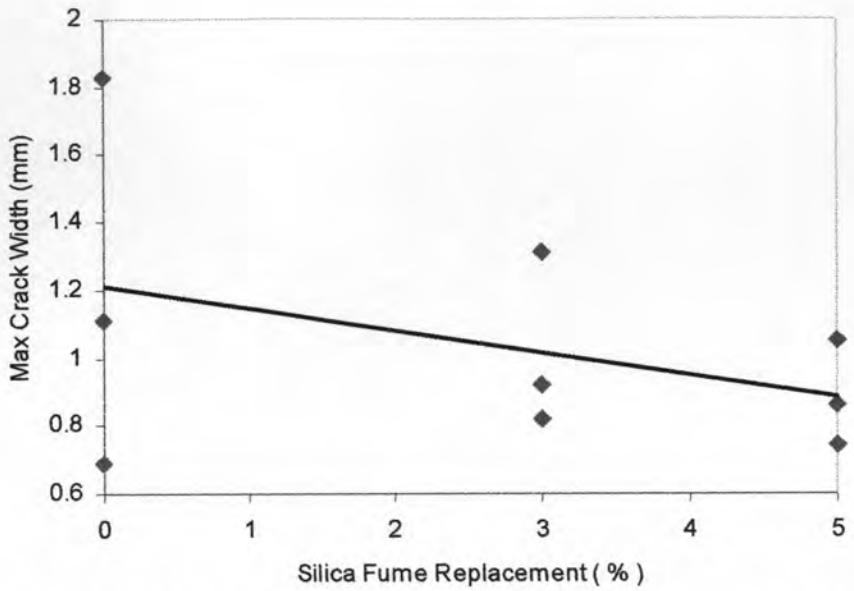

Figure 4.33: Effect of silica fume content on maximum crack width

The 90 percentile plastic shrinkage crack widths, shown in Table 4.14, were determined using the same methods utilized in fly ash concrete. Ninety percent of crack widths would not be greater than the values tabulated. It was noticed that the values from either normal distribution or sorting were almost the same (having only a 1 percent difference for the 50-5SF specimens). Once again, this has shown that the crack width measurements were normally distributed. Similar to the limiting crack widths determined for fly ash concrete, it was observed that the values in Table 4.14 also exceed the tolerable crack width values suggested by ACI 224 for different exposure conditions Additional precautions must then be used when using silica fume concrete to control or reduce other possible permeability problems caused by plastic shrinkage cracks due to different exposure conditions..

Table 4.14: Ninety percentile crack width values of silica fume concrete specimens

Designation	90 Percentile Crack Width Values	
	Normal	Sort
w/b-%SF	mm	mm
50-C	1.09	1.09
50-3SF	0.82	0.82
50-5SF	0.69	0.68

4.2.4 Effect on Crack Area

The observed decrease in the values of both calculated average and measured maximum crack widths showed that the use of silica fume in concrete would also result in a decrease in the plastic shrinkage crack area. As shown in Figure 4.34, crack area decreased as the amount of silica fume used increased. Even though there was a very significant decrease in bleed water which would supposedly increase plastic shrinkage, the micro filler effect of silica fume particles was still the main parameter that caused the decrease in the quantification values of plastic shrinkage cracks. The theory of the effect of paste stiffness on plastic shrinkage crack area of Wang, Shah, and Phuaksuk (2001) does not apply to silica fume concrete. Even as the increase of silica fume used in the concrete allowed it to be less workable than control specimens with the same water/binder ratio, the lesser crack area it produced.

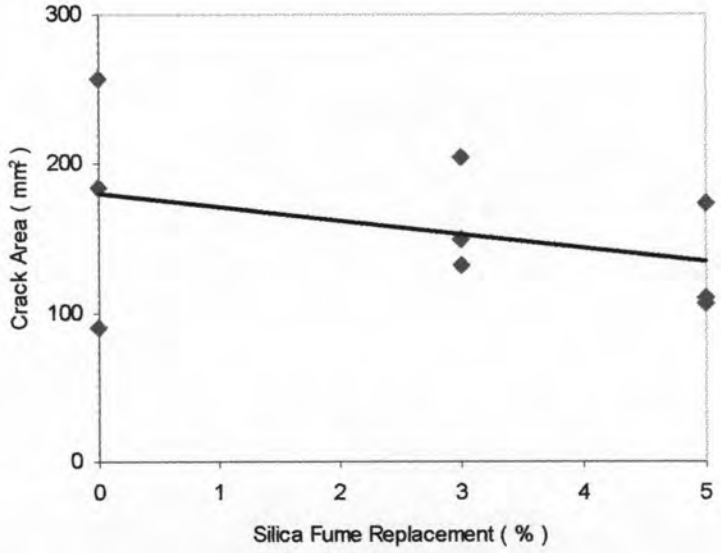

Figure 4.34: Effect of silica fume content on crack area

4.2.5 Effect of Curing on Silica Fume Concrete

As in the case for fly ash concrete specimens, one silica fume specimen per curing condition would be investigated. The crack width measurements were noted before and after curing, as shown in Table 4.15. Day 1 represented the crack

quantification values of the specimen that was chosen to undergo curing after the plastic shrinkage cracking test procedure. Day 28 corresponded to the quantification values of the cracks after chosen specimens have been exposed to curing conditions for 28 days.

Table 4.15: Number of crack width measurements of silica fume concrete specimens for curing

Designation	Number of Data Points			
	Air Curing		Moist Curing	
	Day 1	Day 28	Day 1	Day 28
50-C	64	63	71	68
50-3SF	70	67	65	65
50-5SF	60	56	76	65

Normal distribution curves of the measured crack widths of specimens chosen to undergo curing for 28 days are shown in Figures 4.35 to 4.36. As observed in fly ash concrete specimens, the curves tend to be displaced to the left after undergoing exposure to curing conditions for 28 days. However, unlike air cured fly ash concrete specimens, there was a significant change that was observed in silica fume concrete specimens that underwent air curing (Figure 4.35). Plastic shrinkage crack widths were reduced even at the absence of additional moisture in air curing. It is still noted that the changes in moist cured specimens, shown in Figure 4.36, were still larger than the observed changes in air cured specimens which implied greater reduction in crack widths due to the additional amount of moisture to further hasten hydration. From these figures, we could see the early age performance of silica fume irregardless of curing conditions.

In addition to this, it was observed that the shape of the normal distribution curve changed in both air cured and moist cured specimens. The decrease in standard deviation values (Table 4.16) after curing indicated that the curve became narrower, thus resulting in crack width values closer to the mean. As a result, the crack width values would be more uniform. Standard deviation was noticed to decrease as the amount of silica fume increased. This implied that the crack width values tend to be more uniform (as it becomes closer to the mean value) as the silica fume content increased. However, standard deviation was greatly reduced after curing (especially

after moist curing). The apparent change in normal distribution shape denoted that the distribution of healing, whether by air curing or moist curing, was non-uniform. Seemingly, narrower crack widths were healed first. The propagation of healing could have started from the edge with the narrowest crack width towards wider cracks. Similarly to what was observed after curing fly ash concrete, smaller gaps could have been easily filled by hydration products first.

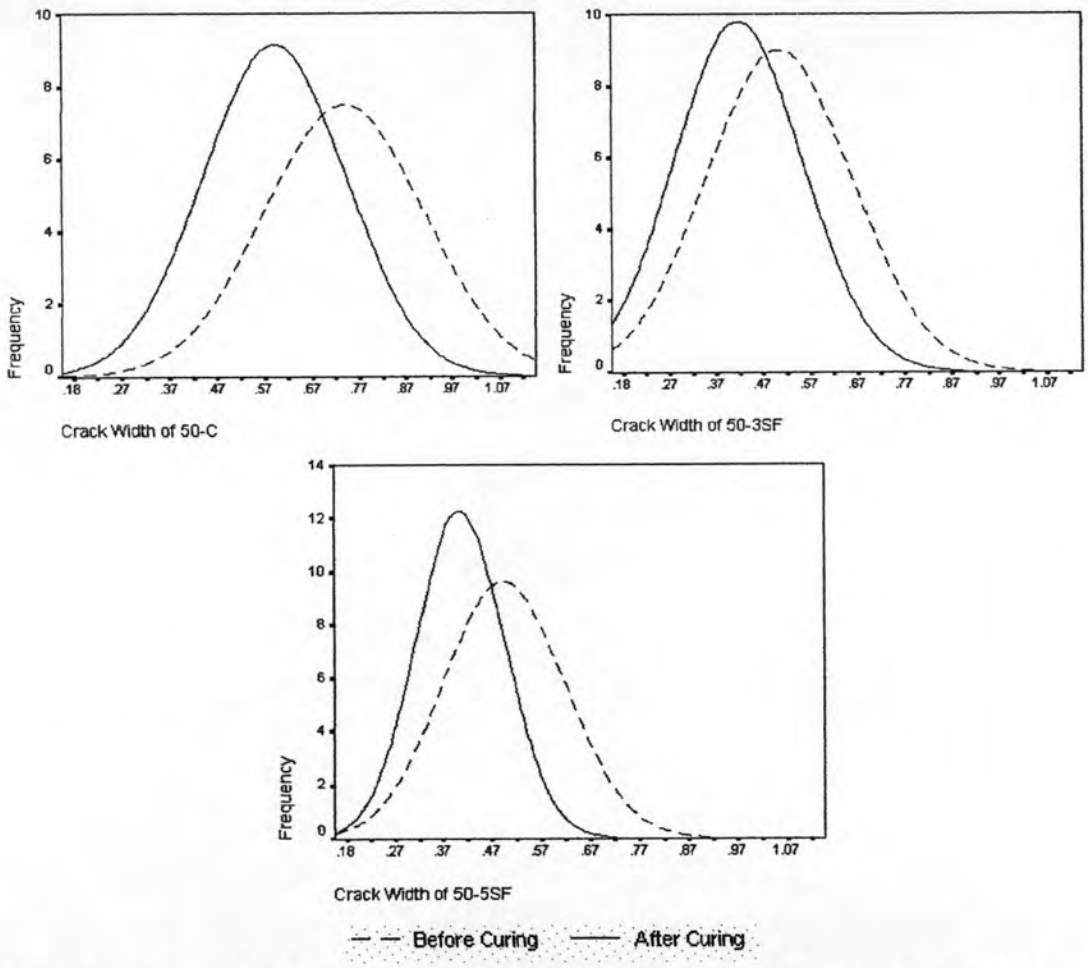

Figure 4.35: Normal distribution curve comparison for silica fume concrete specimens under air curing conditions

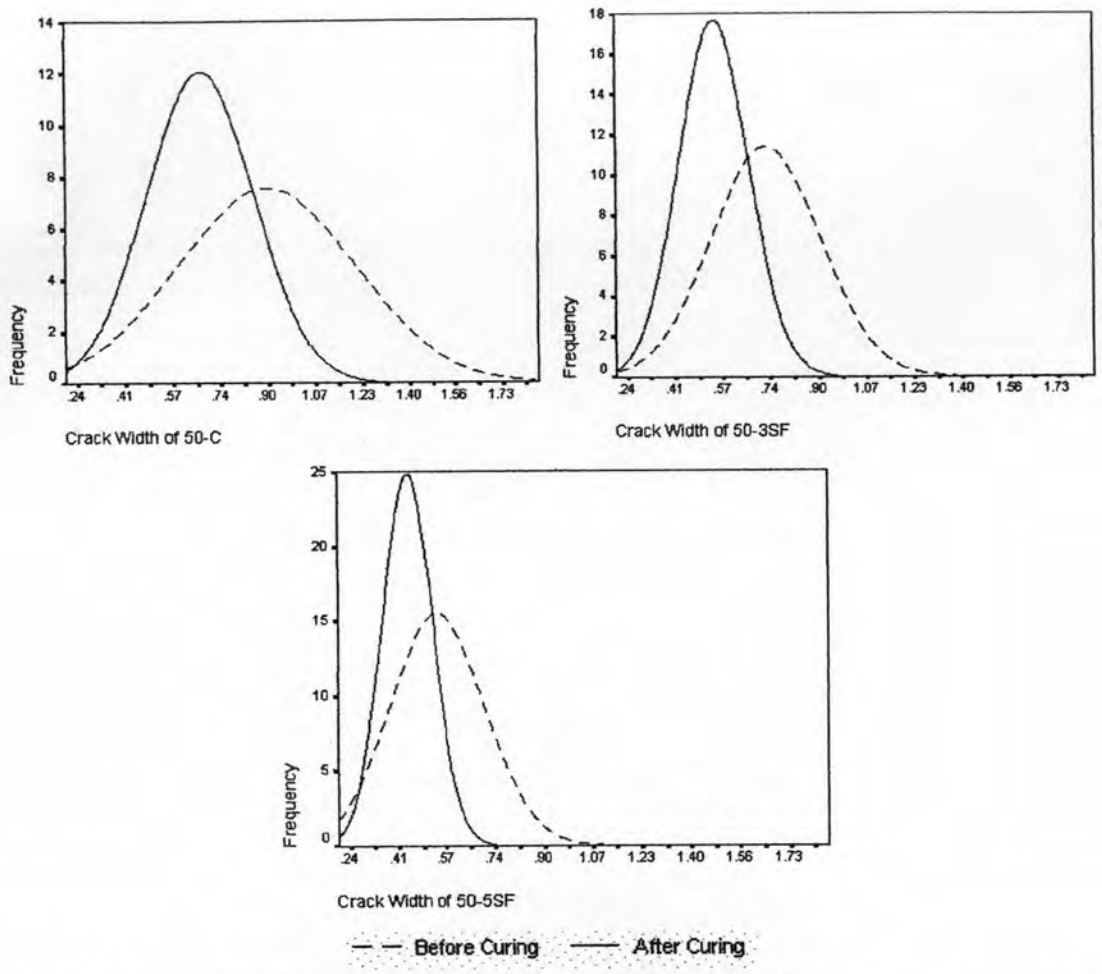

Figure 4.36: Normal distribution curve comparison for silica fume concrete specimens under moist curing conditions

Table 4.16: Standard deviation values of cured silica fume concrete specimens

Designation	Standard Deviation			
	Air Curing		Moist Curing	
	Day 1	Day 28	Day 1	Day 28
50-C	0.170	0.151	0.309	0.185
50-3SF	0.155	0.136	0.187	0.121
50-5SF	0.124	0.091	0.161	0.086

The observed behaviors from the normal distribution curve plots would be further strengthened using results from linear regression analysis. As discussed in Section 4.1.5, the greater the positive calculated value to percent change would be, the greater the reduction of crack quantification values. The greater the reduction in crack quantification values, the more effective the curing condition had been in reducing plastic shrinkage cracking of concrete.

Even though that there was a detected decrease in the percent change in average crack width (Figure 4.37), the high increase in percent changes in both maximum crack width (Figure 4.38) and crack area (Figure 4.39) as the amount of silica fume increased has shown the innate properties of silica fume. These properties were early pozzolanic reaction and micro filler effect. The micro filler effect of the ultrafine silica fume particles permitted the decrease in crack width and crack area. Its early pozzolanic reaction allowed for further reduction in plastic shrinkage cracks thru the healing properties of silica fume concrete which was enhanced by curing. Such claim was supported by high percentage changes (all positive values) shown in Figures 4.37 to 4.39. The percent change of moist cured silica fume concrete specimens has proven the effectiveness of moist curing in enhancing hydration that would further help in the reduction of plastic shrinkage cracks.

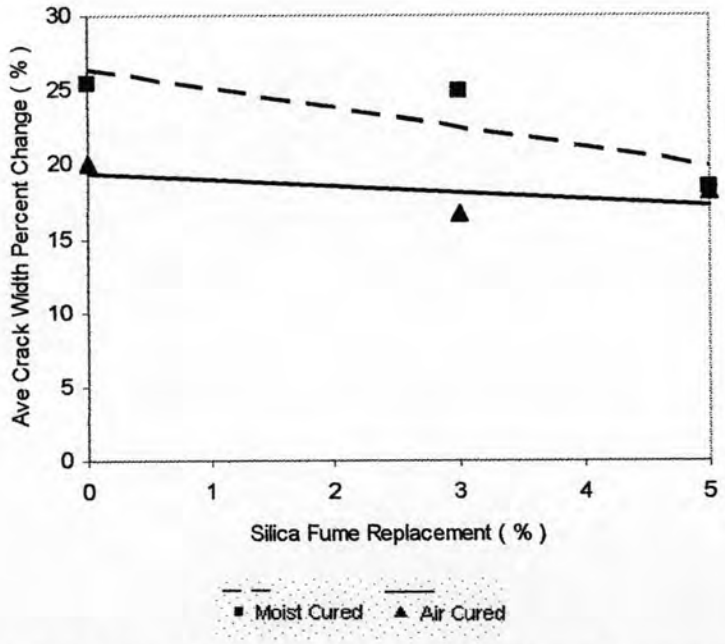

Figure 4.37: Effect of silica fume content on percent change in average crack width

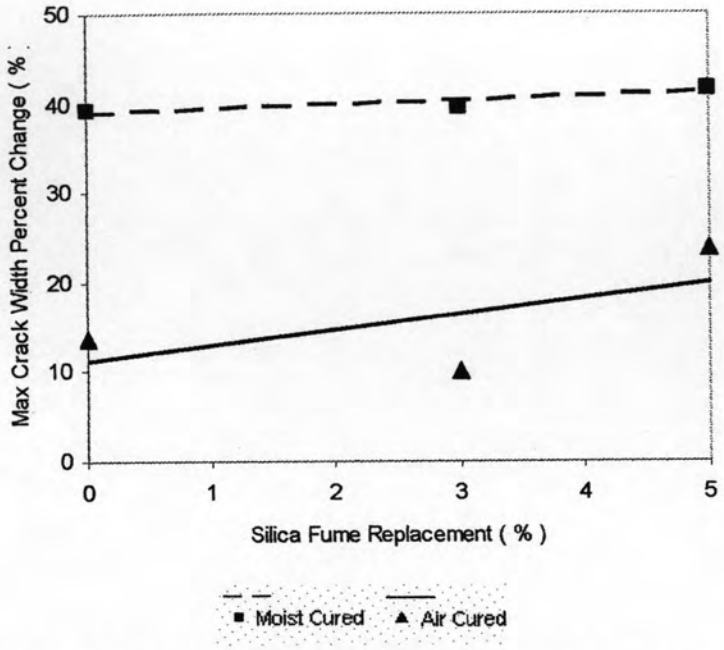

Figure 4.38: Effect of silica fume content on percent change in maximum crack width

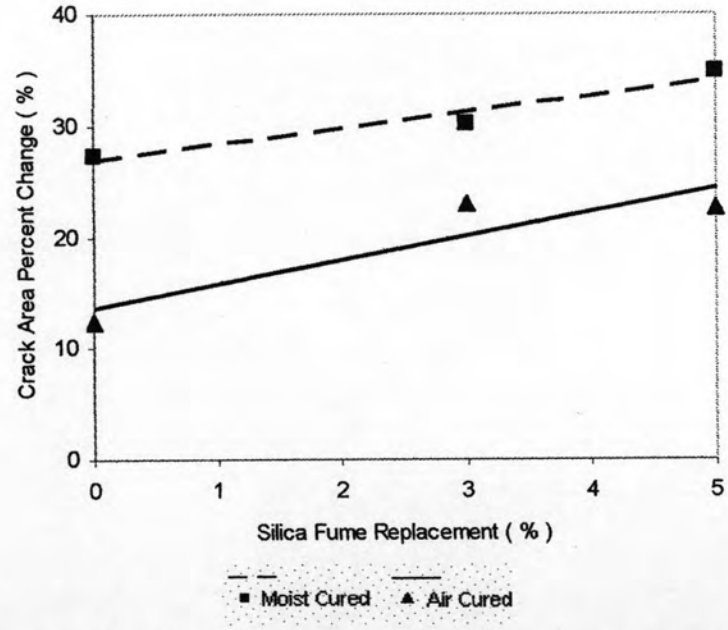

Figure 4.39: Effect of silica fume content on percent change in crack area

As compared to the percentage values of fly ash concrete specimens, the percent change of the calculated crack quantification values of silica fume concrete was still greater. Perhaps such behavior could be attributed to the property of silica

fume to enhance early age properties of concrete while fly ash enhances properties of concrete at a later age.

In terms of the ninety percentile plastic shrinkage crack widths after curing (Table 4.17), it was observed that the values still exceeded the tolerable crack widths seen in Table 4.5. Moreover, the mean crack widths for either air or moist cured specimens (Table 4.17) also exceeded tolerable crack width values except for the 50-5SF specimens. After 28 days of being air cured, it was found that using 5 % replacement of cement by silica fume using water/binder ratio of 0.50 could possibly survive dry air exposure conditions by 50 percent. Having only a slight difference, it is possible that the tolerable crack width for dry air exposure could be attained also with the use of 50-5SF mixes and moist curing. It is promising or likely that with the previously observed behavior of silica fume concrete, further increase in silica fume content as cement replacement with water/binder ratio of 0.50 could possibly attain the tolerable crack width values for dry air or even moist air exposure conditions with the aid of either air or moist curing conditions.

Table 4.17: Ninety percentile crack width values of chosen silica fume concrete specimens after curing

Designation	90 Percentile Crack Width							
	Air Curing				Moist Curing			
	Day 1		Day 28		Day 1		Day 28	
	Normal	Sort	Normal	Sort	Normal	Sort	Normal	Sort
w/b-%SF	mm	mm	mm	mm	mm	mm	mm	mm
50-C	0.96	0.96	0.77	0.77	1.35	1.29	0.92	0.92
50-3SF	0.73	0.69	0.62	0.59	0.97	0.97	0.72	0.70
50-5SF	0.67	0.67	0.50	0.50	0.79	0.76	0.53	0.53

Table 4.18: Mean crack width values of chosen silica fume concrete specimens after curing

Designation	Mean Crack Width			
	Air Curing		Moist Curing	
	Day 1	Day 28	Day 1	Day 28
w/b-%SF	mm	mm	mm	mm
50-C	0.744	0.596	0.897	0.668
50-3SF	0.508	0.422	0.719	0.541
50-5SF	0.499	0.410	0.537	0.436

4.2.6 Cracking Reduction Ratio of Silica Fume Concrete

The reduction in average crack width, maximum crack width, and crack area of plastic shrinkage has shown very promising behavior of silica fume concrete in terms of its effectiveness in reducing plastic shrinkage cracks. This claim was strengthened by the trend shown in Figure 4.40. An increase in silica fume content would further reduce the average plastic shrinkage crack widths. From the figure, even a 1% silica fume replacement of cement could render reduction in average crack widths since analysis have shown that cracking reduction ratio was above the zero mark. Due to this trend, it is possible that further increase in silica fume content would allow silica fume concrete to be less vulnerable to any exposure condition in terms of plastic shrinkage cracks.

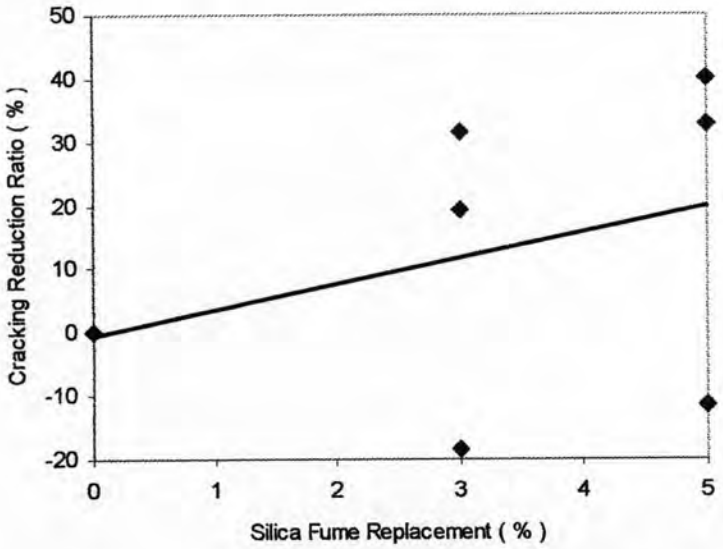

Figure 4.40: Effect of silica fume content on cracking reduction ratio

From the analysis done on both silica fume and fly ash concrete, it could be said that the use of silica fume is more effective in reducing plastic shrinkage cracks. Increasing the amount of silica fume in concrete reduces average crack width, maximum crack width, and crack area. One disadvantage that might be critical is that the use of silica fume in concrete is more expensive than just using fly ash.

4.2.7. Summary of Results of Silica Fume Concrete

Average crack width, maximum crack width, and crack area decreased as the amount of silica fume increased in concrete with high water/binder ratio of 0.50. Also, it was observed that as silica fume content increased, the effectiveness in plastic shrinkage crack reduction in terms of the cracking reduction ratio also increased. Such behavior of silica fume concrete specimens could be seen in Figure 4.41. It was also observed that the reduction in plastic shrinkage cracks was greater in specimens that were exposed to moist curing conditions for 28 days than in air curing conditions. This has shown that moist curing would further reduce plastic shrinkage cracks in silica fume concrete.

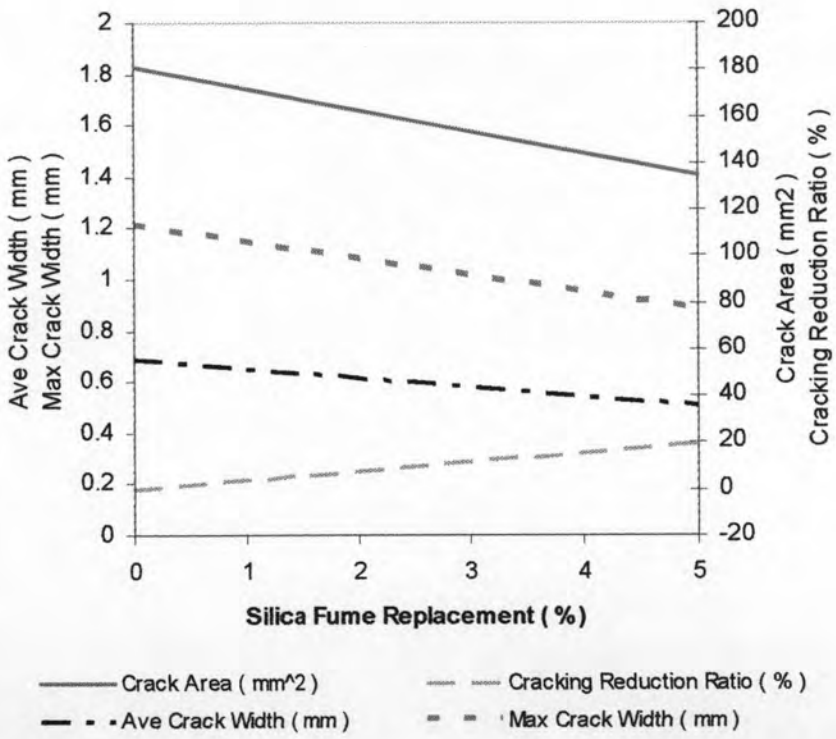

Figure 4.41: Effect of silica fume content on average crack width, maximum crack width, crack area and cracking reduction ratio